Critical Evaluation of Potentiostatic Holds as Accelerated Predictors of Capacity Fade during Calendar Aging

Maxwell C. Schulze,[1,=] Marco-Tulio F. Rodrigues,[2,=] Josefine D. McBrayer,[3,4,=] Daniel P. Abraham,[2] Christopher A. Apblett,[3] Ira Bloom,[2] Zonghai Chen,[2] Andrew M. Colclasure,[5] Alison R. Dunlop,[2] Chen Fang,[6] Katharine L. Harrison,[7] Gao Liu,[6] Shelley D. Minteer,[4] Nathan R. Neale,[1] David Robertson,[2] Adam P. Tornheim,[2] Stephen E. Trask,[2] Gabriel M. Veith,[8] Ankit Verma,[5] Zhenzhen Yang,[2] and Christopher Johnson[2,**,z]

[1]*Materials, Chemical, and Computational Science, National Renewable Energy Laboratory, Golden, CO, United States of America*
[2]*Chemical Sciences and Engineering Division, Argonne National Laboratory, Lemont, IL, United States of America*
[3]*Power Sources Technology Group, Sandia National Laboratory, Albuquerque, NM, United States of America*
[4]*Department of Chemistry and Chemical Engineering, University of Utah, Salt Lake City, UT, United States of America*
[5]*Energy Conversion and Storage Systems Center, National Renewable Energy Laboratory, Golden, CO, United States of America*
[6]*Energy Storage and Distributed Resources Division, Lawrence Berkeley National Laboratory, Berkeley, CA, United States of America*
[7]*Nanoscale Sciences Department, Sandia National Laboratory, Albuquerque, NM, United States of America*
[8]*Chemical Sciences Division, Oak Ridge National Laboratory, Oak Ridge, TN, United States of America*

Li-ion batteries will lose both capacity and power over time due to calendar aging caused by slow parasitic processes that consume Li^+ ions. Studying and mitigating these processes is traditionally an equally slow venture, which is especially taxing for the validation of new active materials and electrolyte additives. Here, we evaluate whether potentiostatic holds can be used to accelerate the diagnosis of Li^+ loss during calendar aging. The technique is based on the idea that, under the right conditions, the current measured as the cell voltage is held constant can be correlated with the instantaneous rate of side reactions. Thus, in principle, these measurements could capture the rate of capacity fade in *real time*. In practice, we show that this method is incapable of quantitatively forecasting calendar aging trends. Instead, our study demonstrates that potentiostatic holds can be applied for initial qualitative screening of systems that exhibit promising long-term stability, which can be useful to shrink the parameter space for calendar aging studies. By facilitating the identification of improved formulations, this approach can help accelerate innovation in the battery industry.

Li-ion batteries (LIBs) are among the most impactful inventions of the 20th century.[1] After revolutionizing the portable electronics industry, LIBs are now key in enabling a wider adoption of electric vehicles (EVs) and the transition towards a greener electric grid. The economic feasibility of both these applications relies heavily on the durability of the battery pack, as the upfront costs of EV ownership and infrastructure investments are only slowly recovered over time.[2,3]

The longevity of LIBs is constantly challenged by the meta-stable nature of the electrochemical processes in the cells. Graphite electrodes operate at potentials beyond the limits of thermodynamic stability of the electrolyte, with the solid electrolyte interphase (SEI) serving as a kinetic barrier to uncontrolled reduction reactions.[4] As effective as the SEI can be in enabling LIB operation, it is not perfect, allowing side reactions to continue at slow but persistent rates. Hence, Li-ion batteries will always lose some amount of charge when at rest, even if they are never actively charged or discharged. The consequences of these time-dependent degradation processes are known as *calendar aging*, and the time needed for such processes to consume 20% of the initial cell capacity is called *calendar life*.[5] Losses of Li^+ inventory due to calendar aging are typically greater during conditions that accelerate the kinetics of parasitic reactions at the SEI, such as elevated temperatures (which increase reaction rate constants) and at lower effective anode potentials (that increase overpotentials for electrolyte reduction).[5–7] Constraining batteries to operate at low temperatures and limited full-cell states-of-charge (SOCs) would naturally delay the course of time-dependent aging, but these are not always practical options, nor are they permanent solutions to the calendar aging problem.

As calendar aging effects on Li^+ inventory are intimately linked with the SEI, they can be mitigated by employing electrode and electrolyte chemistries that yield more robust SEI layers.[8] Although materials discovery is always a complex and lengthy endeavor, new battery chemistries can be especially difficult to develop when the mere evaluation of any formulation change requires long-term experimentation. Since calendar aging is intrinsically slow, studies typically alternate between long-term storage (~1 month) and brief reference performance tests (RPTs), which can involve cycling at slow rates and impedance measurements that are used to quantify the time-dependent performance degradation.[9] Thus, capturing meaningful trends from these tests requires resource-intensive studies that can extend for many months or years. A common approach to accelerate these studies is to maintain cells at higher temperatures where the effects of aging are accelerated. However, it is always a challenge to ensure that trends observed at elevated temperatures remain valid at the milder operating conditions that batteries typically experience,[10] and even these accelerated tests still require many months to be completed.[5,7]

The lengthy iterative process needed to improve calendar life is especially problematic for new technologies, as is the case for silicon anodes. Silicon is much more reactive towards the electrolyte and

[=]These authors contributed equally to this work.
*Electrochemical Society Fellow.
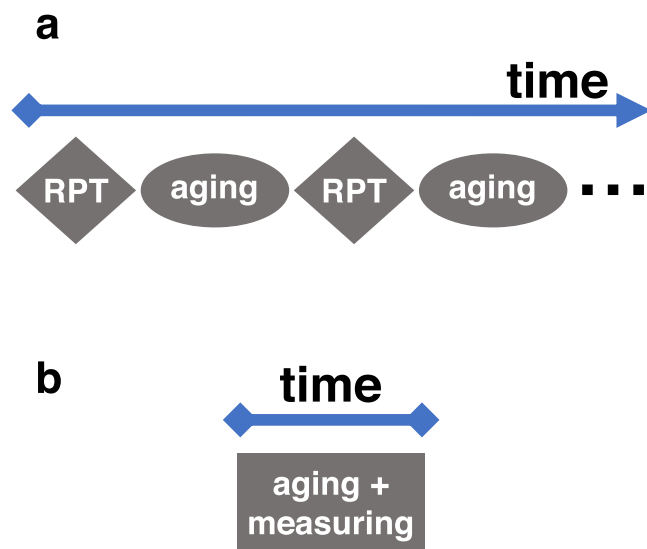[z]E-mail: cjohnson@anl.gov

a

b

Figure 1. Conceptualizing an ideal accelerated calendar aging experiment. (a) Traditional experiments alternate periods of aging at open circuit voltage and reference performance tests (RPTs) that quantify the performance loss. Typically, month-long storage periods are repeated for a year or more to sufficiently resolve the time dependency of calendar aging. The vast majority of the time is spent aging the cells, rather than measuring its consequences. (b) Test duration could be expedited if aging and measurement of the resulting capacity loss were performed simultaneously. The enhanced time resolution for information acquisition could drastically shorten calendar aging experiments.

unravel the underlying mechanisms and identify strategies for their mitigation. A core point that could benefit such explorations, both by academic groups and by manufacturers, is the development of experimental approaches that can expedite calendar aging experiments to accelerate the innovation process. In the present work, we discuss the merits and limitations of *potentiostatic holds* as one such expedient method.

One characteristic of traditional calendar aging studies is that aging and the measurement of its consequences exist as separate steps. Considering that a typical aging experiment involves 1 month of inactive storage and less than 3 d of active RPT measurement, less than 10% of the total time of these tests are invested in acquiring information that will be used to evaluate cell behavior. In other words, a full month of testing will yield a single data point. One fundamental way to decrease the total test time would be to simultaneously age the cell *and* measure its capacity loss, converting the entire experiment into an active process. Moreover, assuming that such measurements could be made with sufficient accuracy, their higher time resolution could make general aging trends apparent much faster than in traditional months-long experiments (Fig. 1).

Potentiostatic holds[15–18] (also known as voltage holds or float tests)[19–21] could, in principle, provide this type of information. In this technique, full-cell voltage is forced to remain constant using an external source while the current needed to maintain the voltage is recorded. It is generally hypothesized that, when certain conditions are met, the measured current can be correlated with the instantaneous rate of parasitic electron exchanges occurring inside the cell, thus providing a picture of the time-dependent trends of these reactions.

The present study compiles extensive analyses on the use of the voltage hold method as an expedient alternative to RPT-based aging studies. We investigate the merits and limitations of the technique, and its applicability to the quantitative, semi-quantitative and qualitative description of calendar aging, using commercial 18650-format cells, single-layer pouch cells, and coin cells. For the reader's benefit, best practices for applying this technique to accelerate the identification of electrodes and electrolytes with enhanced long-term stability are summarized in the final section of this article. We expect this initial exploration to provide the battery community with useful

other cell components than traditional graphite electrodes,[11–13] which can exacerbate problems with calendar aging. Indeed, recent data from companies working at developing Si-rich anodes suggests that high-energy Si cells (>300 Wh kg^{-1}) tend to present particularly low calendar lifetimes, suggesting that this is the main technical barrier preventing near-term commercialization of LIBs with high Si content.[14] The U.S. Department of Energy (DOE) has recognized this problem as a strategic challenge and has allocated resources to

Table I. Electrode composition and basic properties. PVDF stands for poly(vinylidene difluoride), and the LiPAA was obtained after partial neutralization of poly(acrylic acid) with LiOH. All electrodes were calendered to the indicated porosity.

Graphite 1 (Gr-1)	Graphite 2 (Gr-2)
91.83 wt% Superior Graphite SLC1506T	91.83 wt% Superior Graphite SLC1520P
2 wt% C45 carbon additive (Timcal)	2 wt% C45 carbon additive (Timcal)
0.17%wt oxalic acid	0.17%wt oxalic acid
6 wt% PVDF binder (KF-9300, Kureha)	6 wt% PVDF binder (KF-9300, Kureha)
37.4% electrode porosity	35.6% electrode porosity
47 μm-thick composite coating	45 μm-thick composite coating
6.49 mg cm^{-2} and 2.1 mAh cm^{-2}	6.28 mg cm^{-2} and 2.0 mAh cm^{-2}
15% Si-Graphite (15% Si-Gr)	**80% Silicon**
73 wt% Hitachi MagE3 graphite	80 wt% 200 nm Si (Paraclete Energy)
15 wt% 200 nm Si (Paraclete Energy)	10 wt% C45 carbon additive (Timcal)
2 wt% C45 carbon additive (Timcal)	10 wt% LiPAA binder (Sigma-Aldrich)
10 wt% LiPAA binder (Sigma-Aldrich)	47.3% electrode porosity
48% electrode porosity	10 μm-thick composite coating
28 μm-thick composite coating	1.10 mg cm^{-2} and 1.5 mAh cm^{-2} (100 mV cutoff)
2.97 mg cm^{-2} and 2.45 mAh cm^{-2} (50 mV cutoff)	
LFP	**NMC622**
90 wt% Johnson Matthey LiFePO$_4$	90 wt% LiNi$_{0.6}$Mn$_{0.2}$Co$_{0.2}$ (Targray)
5 wt% C45 carbon additive (Timcal)	5 wt% C45 carbon additive (Timcal)
5 wt% PVDF binder (5130, Solvay)	5 wt% PVDF binder (5130, Solvay)
38.8% electrode porosity	37.1% electrode porosity
98 μm-thick composite coating	58 μm-thick composite coating
19.70 mg cm^{-2} and 2.66 mAh cm^{-2}	9.78 mg cm^{-2} and 1.58 mAh cm^{-2} (3–4.3 V)

tools to expedite the development of battery technology. For the interested reader, additional detailed discussion is provided in the Supplementary Material.

Experimental

Materials and methods.—The composition of all electrodes used in this work is detailed in Table I. Electrodes were dried overnight under dynamic vacuum at 120 °C (for PVDF binder) or 150 °C (for LiPAA binder) prior to use. Most tests with lab-scale cells used Gen2 electrolyte (1.2 M LiPF$_6$ in a 3:7 wt:wt mixture of ethylene carbonate and ethyl methyl carbonate) with 10 wt% fluoroethylene carbonate (FEC). Certain tests used Gen2 containing 2 wt% vinylene carbonate (VC), 2 wt% ethylene sulfite (ES) and 2 wt% tris(tri-methylsilyl) phosphite (TMSPi); usage of Gen2 + VC/ES/TMSPi is explicitly acknowledged. Gen2 and FEC were procured from Tomiyama and Solvay, respectively. TMSPi and ES were purchased from Sigma Aldrich, while VC was acquired from TCI America. All electrolyte components were used as-received.

Coin cells.—2032-format cells used 14 mm and 15 mm electrodes, a 19 mm Celgard 2325 separator, two 0.5 mm thick stainless steel spacers, and a stainless steel wave spring. In full-cells, the anode was the larger electrode; in half-cells, the Li electrode was larger. 40 μl of electrolyte was added to each cell, corresponding to at least 4x the total pore volume of electrodes and separator for all systems. The electrolyte was either Gen2 + FEC or Gen2 + VC/ES/TMSPi. The identity of electrodes used in each case is explicitly acknowledged in the text, and the detailed composition can be found in Table I. LFP-based cells were formed at a rate of C/10 between 2.7–3.42 V for Gr cells and 2.7–3.35 V for silicon-containing cells. Voltage holds were performed at either 3.35 or 3.335 V. NMC-based cells were cycled at C/10 between 3.0 and 4.1 V, and were aged at open circuit after a full charge. Cycling tests and voltage holds were performed on Maccor 4100 cyclers at 30 °C or at the indicated temperature.

Single-layer pouch cells.—The xx3450-format cells were pre-pared using 14.1 and 14.9 cm^2 electrodes. An "overhang" is typically reserved for the anode, to reduce the likelihood of local anode overcharge due to electrode edge effects such as potential gradients, concentration gradients, or assembly imperfections such as electrode misalignment. Here, cells with both cathode and anode overhangs are explored to probe the effect of these excess areas on
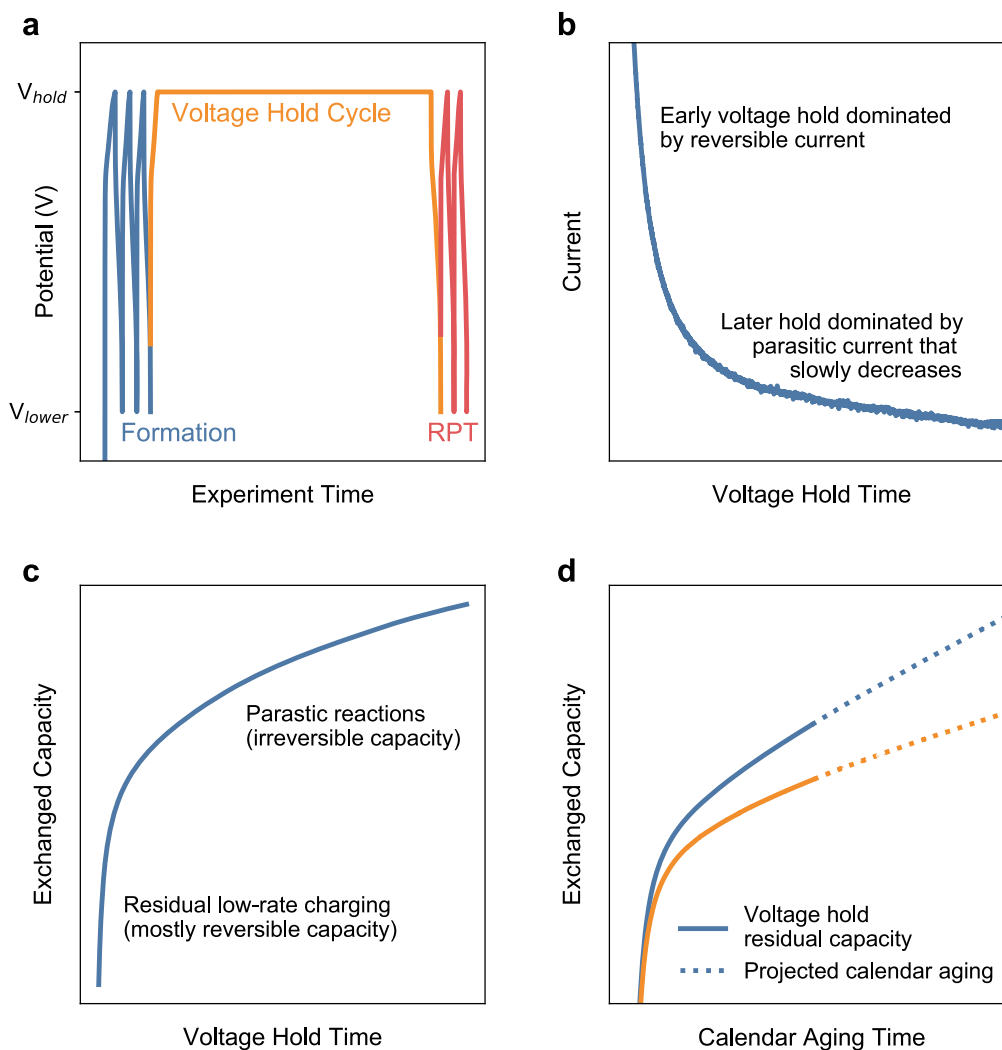

Figure 2. (a) Typical voltage vs time profile of a voltage hold experiment. (b) The current response measured during the voltage hold period comprises contributions from reversible processes that dominate early in the hold and parasitic process that irreversibly consume Li$^+$-inventory but slowly decrease as the SEI matures and becomes more passivating. (c) Integration of the current response during the voltage hold yields the exchanged capacity. The significant rise early in the testing period is due to residual low-rate charging of the cell (reversible processes) while the shallower profile later in the hold is more representative of the irreversible processes that affect the cell's calendar lifetime. (d) The time dependent behavior of irreversible capacity measured during the voltage hold could *potentially* be extrapolated into the future to predict the calendar aging behavior of a cell, assuming Li$^+$ inventory loss at the anode as the sole calendar aging mechanism. The blue and orange curves represent examples of faster and slower degradation, respectively.

the outcome of voltage hold experiments. A total of four types of cells were prepared: (i) LFP vs Gr-1 (anode overhang); (ii) LFP vs Gr-1 (cathode overhang); (iii) LFP vs 15% Si-Gr (anode overhang); and (iv) LFP vs 15% Si-Gr (cathode overhang). Four cells of each type were assembled. Note that these cells had a N/P ratio < 1, as the excess Li^+ inventory allows long-term voltage holds at high SOCs to be performed (see text below for details). Celgard 2325 was used as the separator, and the electrolyte was Gen2 + 10 wt% FEC. The electrolyte volume added to each cell was equivalent to ∼4x the total pore volume of electrodes and separator. The formation protocol included three C/10 cycles between 2.7–3.42 V for Gr cells, and 2.7–3.35 V for Si-Gr cells; at 3.35 V the anode experiences ∼100 mV vs Li/Li$^+$, thus limiting the extent of Si expansion. Cells were degassed and resealed after the formation cycles. Voltage holds were performed at 3.335 V and 30 °C for various periods on either a Maccor 4100 or a custom-made high-precision cycler.

Cylindrical cells.—18650-format cylindrical cells were acquired from LithiumWerks (formerly A123). The cell model used was Nanophosphate® APR18650M1-B, which has a graphite anode and LFP cathode matched for the cell to nominally deliver 1.1 Ah of capacity when cycled between 2.0–3.6 V. Cells were tested immediately when received or refrigerated for future use. Voltage holds were performed at a variety of potentials as specified in the text.

Results and Discussion

Description of the voltage hold technique for studying calendar aging.—There are numerous reports of voltage hold methods in the literature,[15–21] and while they vary in the exact electrochemical protocol used, they have common elements. Figure 2a shows an example potential profile of a voltage hold protocol that can be broken down into the three main parts shown in Fig. 1b. The formation is typically a series of slow cycles used to form the SEI (formation) and to measure the beginning-of-life electrochemical behavior and performance of the cell. The voltage hold cycle that follows typically charges the cell up to a hold potential (V_{hold}), holds at that potential for some time, then discharges the cell. In some cases, an RPT comprising a few cycles is run after the hold cycle to help gather more diagnostic electrochemical information.

The basis of using such a voltage hold experiment to learn about calendar aging of the cell centers on analyzing the current response measured during the voltage hold, an example of which is shown in Fig. 2b. The current response comprises contributions from both reversible (I_{rev}, charging) and irreversible (I_{irrev}, parasitic reactions) processes. The reversible processes arise from continuous charging of the cell as the current decreases, as depolarization makes additional capacity available at V_{hold}. Over time, these reversible processes should relax to negligible levels as the cell equilibrates to a constant SOC, and the irreversible processes should start to dominate the current response.[18] Thus, the current response of a sufficiently long voltage hold could ideally be used to measure the rate of irreversible parasitic reactions in a cell at a constant SOC. Integration of the current response yields the capacity exchanged during the voltage hold (Q_{hold}) as shown in Fig. 2c. Here, the early rise in Q_{hold} is primarily from continued reversible charging (Q_{rev}) of the cell, with the irreversible capacity (Q_{irrev}) represented by the smaller slope later in the hold. Q_{hold} can thus be represented by the following time dependent function:

$$Q_{hold}(t) = Q_{irrev}(t) + Q_{rev}(t) \qquad [1]$$

In principle, data curves like that shown in Fig. 2c could describe the time-dependence of side reactions in the cell. If such measurements are sufficiently accurate, and if losses of Li^+ inventory occur at much higher rates than other aging modes, these tests *could hypothetically* be used to infer the functional form of $Q_{irrev}(t)$ and

extrapolate the future capacity loss of the cell (Fig. 2d). While this type of extrapolation oversimplifies the complex processes involved in calendar aging, it could potentially serve as an accelerated method for predicting calendar aging behavior of a cell without using the lengthy RPT-based experiments depicted in Fig. 1a. Additionally, the time resolution with which the rate of parasitic processes could be described could be useful in supporting the development of electrochemical models able to capture the interplay of the slow processes responsible for calendar aging. These potential benefits have motivated our detailed exploration of this technique. As we demonstrate below, while these optimistic expectations were not fulfilled, the technique still proved useful for the study of calendar aging.

The calendar aging of batteries occurs by any number of mechanisms, including the irreversible loss of Li^+ inventory (Q_{loss}) to the anode SEI, impedance rise due to buildup of SEI at the anode, oxygen loss and rock-salt formation in the cathode,[22,23] side reactions at the cathode surface, or excessive electrolyte consumption (also referred to as cell dry-out).[6,14] All these mechanisms are fundamentally caused by parasitic processes between the electrolyte and electrodes, so measuring the time dependency of those parasitic reactions provides information about their individual contributions to calendar aging.[17,24] Because the loss of Li^+ to the SEI is the main mechanism of capacity fade during calendar aging of commercial cells,[25] our work emphasizes this particular aging mode. Our examples also focus specifically on voltage holds of graphite and silicon anodes, due to their ubiquity and high chemical reactivity,[11,12] respectively. Both graphite and silicon form an SEI and operate at low potentials outside of the electrolyte stability window which makes them susceptible to calendar aging. However, properly passivated graphite typically has good calendar life while the innate reactivity of silicon leads to rapid degradation over time.

For this type of methodology to be valid, the voltage hold must be run under conditions where $Q_{rev}(t)$ saturates into a constant value ($\partial Q_{rev}(t)/\partial t = I_{rev} = 0$), so the measured I_{irrev} ($\partial Q_{irrev}(t)/\partial t$) corresponds to the rate of parasitic reactions at the anode; that is:

$$\partial Q_{hold}(t)/\partial t = \partial Q_{irrev}(t)/\partial t. \qquad [2]$$

An essential requirement is that the SOC of the anode must remain fixed so that the measured current corresponds only to parasitic current, rather than also comprising reversible contributions from a changing anode SOC. Continuous lithiation of the anode would cause the measured current to be larger than I_{irrev}, while a decrease in anode SOC over time would cause the current to be smaller than I_{irrev} (see discussion in section S1). A constant SOC can be maintained in a 3-electrode cell, where the anode potential can be independently held constant vs a stable reference electrode. However, during a voltage hold of a two-electrode cell, the counter electrode only serves as a stable reference electrode if its potential is relatively constant (insensitive) during the entire voltage hold. While a lithium metal foil used in the standard "half-cell" configuration could possibly serve as such a stable counter and reference electrode for a voltage hold, continuous chemical reactions between the Li metal and the electrolyte can impart complicating factors to the results of the experiment.[26] Instead, a cathode such as lithium iron phosphate (LiFePO$_4$, LFP) is an ideal counter/reference electrode for a voltage hold because it delivers most of its capacity at a potential near ∼3.45 V vs Li/Li$^+$.

Figure 3 shows why a counter electrode with a "flat" voltage profile allows the SOC of a hypothetical anode (Si, in this example) to remain constant during a voltage hold, assuming the cell is fully relaxed; the effect of relaxation on voltage holds is discussed in detail below. In these examples, it is important to understand that irreversible capacity loss due to Li^+ inventory consumption by side reactions at the anode causes its voltage profile to capacity-shift relative to the cathode's voltage profile.[27] This capacity-shifting is a consequence of a changing cathode SOC (as a Li^+ and corresponding electron are extracted from the cathode and transferred to
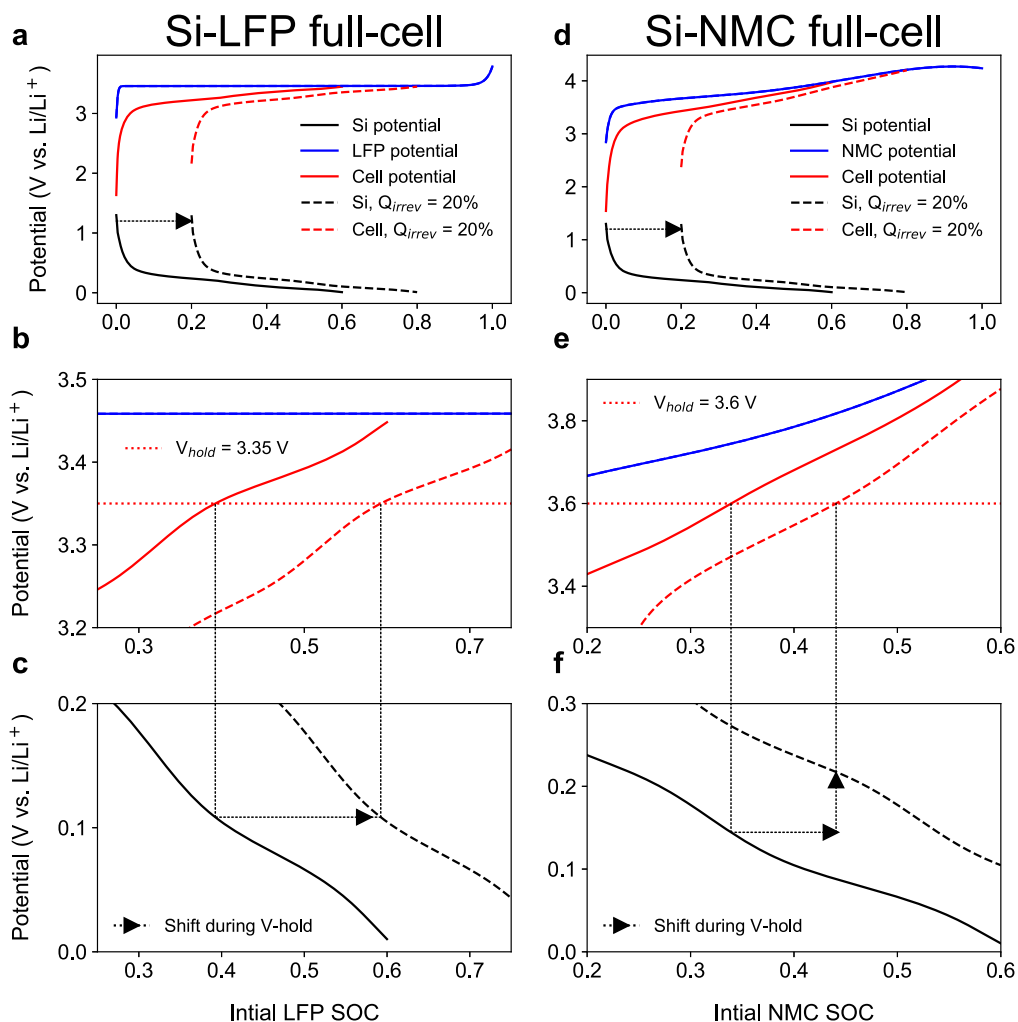
Figure 3. (a) Potential profiles of a Si-LFP full-cell before and after a voltage hold where Q_{irrev} = 20%. The correspondence between the Si-LFP full-cell potential profiles (b) and the Si anode potential profiles (c) before and after the voltage hold at 3.35 V are also shown. (d) Potential profiles of a Si-NMC full-cell before and after a voltage hold where Q_{irrev} = 20%. The correspondence between the Si-NMC full-cell potential profiles (e) and the Si anode potential profiles (f) before and after the voltage hold at 3.6 V are also shown.

the anode) while the anode SOC remains the same (due to the Li^+ and electron being consumed by the parasitic side reaction). Using an LFP cathode as an example of an ideal cell setup for voltage holds, Fig. 3a shows the simulated voltage profiles of an Si-LFP full-cell and how they shift due to irreversible Li^+ inventory loss during a simulated voltage hold. In this ideal cell setup, the Si anode capacity is just 60% of the available Li-inventory supplied by the LFP cathode. Thus, a hypothetical Q_{irrev} = 20% during a simulated voltage hold at 3.35 V is fully accommodated by the excess Li^+ inventory supplied by the LFP. Such configurations with N/P ratio < 1 have been used in the past for diagnostic purposes.[28,29] When the cell potential is held at a constant 3.35 V (Fig. 3b), the Si anode potentials remain nearly unchanged before and after the voltage hold (Fig. 3c), despite 20% of the LFP's Li^+ inventory being consumed in parasitic side reactions at the anode. This is a consequence of the fact that additional LFP capacity can be accessed with negligible variation in cathode potential. Thus, as the cell voltage is held constant, the anode potential will also remain constant as electrons flow from the cathode to the anode to compensate for the side reactions. This implies that any capacity exchanged through the external circuit during the voltage hold is due exclusively to those irreversible reactions, and thus the technique could potentially be used as a predictor of calendar aging behavior.

To highlight the importance of the voltage profile of the counter electrode, Fig. 3d shows the simulated voltage profiles of a Si-NMC811

full-cell and how they shift due to a 20% irreversible Li^+ inventory loss at the Si anode during a simulated voltage hold. In contrast to the Si-LFP full-cell, a Si-NMC full-cell is a non-ideal setup for voltage holds due to the "sloped" voltage profile of the NMC counter electrode, even if the Si anode capacity is just 60% of the available Li^+ inventory supplied by the NMC cathode. To better understand this, Fig. 3e shows how holding the cell potential at a constant 3.6 V corresponds to the Si anode potentials in Fig. 3f, which indicates a rise in the Si anode's potentials (a decrease in the Si SOC, $Q_{Si,\Delta SOC}$) during the voltage hold. In contrast to LFP, accessing additional NMC capacity requires an increase in cathode potential, and it becomes impossible to maintain both the cell voltage and the anode potential invariant. This implies that capacity exchanged during a voltage hold in a Si-NMC cell is a convolution of the irreversible reactions responsible for calendar aging and the change in SOC of the Si anode:

$$Q_{irrev} = Q_{hold} - Q_{Si,\Delta SOC} \qquad [3]$$

Thus, unless the value of $Q_{Si,\Delta SOC}$ can be determined by some independent methods, a voltage hold in a Si-NMC cell will underestimate its instantaneous rate of side reactions. This is a consequence of the "sloped" voltage profile of NMC cathodes and applies to any counter electrode with a "sloped" profile. This also explains why an ideal Si-LFP cell undergoing a voltage hold can underestimate calendar aging rates if Q_{irrev} is large enough that Li^+

inventory supplied by the LFP is fully exhausted and its voltage profile becomes steeply sloped as it polarizes to high potentials (see profile in Fig. 3a, for example). A detailed analysis of how test conditions affect the correspondence between measured and actual parasitic currents is provided in section S1.

Even if a voltage hold is run on a cell that meets the requirements for keeping the anode at a fixed SOC, there are additional assumptions that must be verified to ensure that the measured current accurately corresponds to the instantaneous rate of parasitic reactions. First, the reversible reactions must relax quickly during the voltage hold, so that the measured currents are dominated by the parasitic reactions. Importantly, this means that the timeframe of SOC-changing reactions must be known so that a voltage hold can be run long enough that those reactions become negligible. Second, the parasitic reactions at the anode responsible for calendar aging must be much more prominent than other electrochemical processes

that can generate current during a voltage hold. Examples of other processes that could contribute to the measured current include reversible self-discharge (via an electrical leakage current or a redox shuttle contaminant) or lithiation of an overhanging portion of an anode that is typical in full-cell configurations (not strictly reversible or irreversible). Similarly, the rate of reactions at the anode SEI must be much larger than that of electrolyte oxidation at the cathode. Finally, the instrumentation used to measure the lower currents during a voltage hold must be sufficiently sensitive to accurately measure the parasitic reactions, which can be diminishingly small. We explore the validity of these assumptions in the following sections.

Influence of current relaxation and reversible capacity on the measured aging rate.—To fully understand how the relaxation of reversible currents (I_{rev}) during a voltage hold and the corresponding reversible capacity (Q_{rev}) impact calendar aging studies, we ran a series of experiments using commercial 18650 cells with graphite (Gr) anodes and LFP cathodes (details in the *Experimental* section). The use of commercially available cells affords us high confidence in reproducible behavior from cell to cell, while the LFP cathodes ensure that voltage holds in these 2-electrode cells keeps the Gr SOC as invariant as possible. As an initial assessment of the relaxation of I_{rev} during a voltage hold, we performed the following experiments. Two sets of 3 cells each underwent the same initial set of three cycles (cycles 1, 2, and 3) at a C/10 rate between 2.0–3.6 V, followed by charging each cell up to a hold potential ($V_{hold} = 3.35$ V). One set was then allowed to age at open circuit voltage (OCV) for 30−, 60−, or 90 d (one cell for each aging time), while the cells in the other set were held at V_{hold} for 30−, 60−, or 90 d. Each cell then completed a RPT of two full cycles (cycles 5 and 6) at a C/10 rate after the aging period. The discharge capacities before and after the aging period can then be used to calculate Q_{loss} and Q_{rev} for each cell:

$$Q_{loss} = \frac{Q_{cycle\ 3\ discharge} - Q_{cycle\ 6\ discharge}}{Q_{cycle\ 3\ discharge}} \quad [4]$$

$$Q_{rev} = (Q_{discharge\ immediately\ after\ hold} - Q_{charge\ immediately\ before\ hold})/Q_{cycle\ 3\ discharge} \quad [5]$$

The $Q_{cycle\ 3\ discharge}$ represents the nominal cell capacity at its beginning-of-life before the aging period, while the $Q_{cycle\ 6\ discharge}$ represents the cell capacity after the aging period. The difference between them is normalized relative to the cell capacity at its defined beginning-of-life ($Q_{cycle\ 3\ discharge}$), so Q_{loss} (and related capacities) can be expressed as a percentage of nominal cell capacity, as they are throughout the remainder of the text. Cycle 6, the final cycle of the reference performance test, was selected to give the most accurate estimate of true loss to minimize any residual rebound of the capacity after the voltage hold or OCV rest.

The values for Q_{loss} (calculated using Eq. 4) are plotted in Fig. 4a and show that the cells that underwent the voltage holds exhibited larger Q_{loss} at all aging times than those aged at OCV. We attribute this accelerated aging rate of the voltage hold cells primarily to their higher SOC during aging (non-negligible Q_{rev} values during voltage hold indicate an increase in cell SOC) compared to the OCV aged cells, a phenomenon commonly observed in many battery systems.[25,30] The differential capacity curves in Fig. 4b demonstrate that the voltage hold cells have lithiated to a higher SOC phase in the Gr (dQ/dV peak indicated by *), reaching *anode potentials* that were ~30 mV lower than experienced by the OCV aged cells despite beginning their aging step at the same cell voltage. The aging potential of 3.35 V was chosen because the cell exhibits a low dQ/dV value at that potential, which was thought to minimize Q_{rev} during the voltage hold. However, depolarization of the cell proved
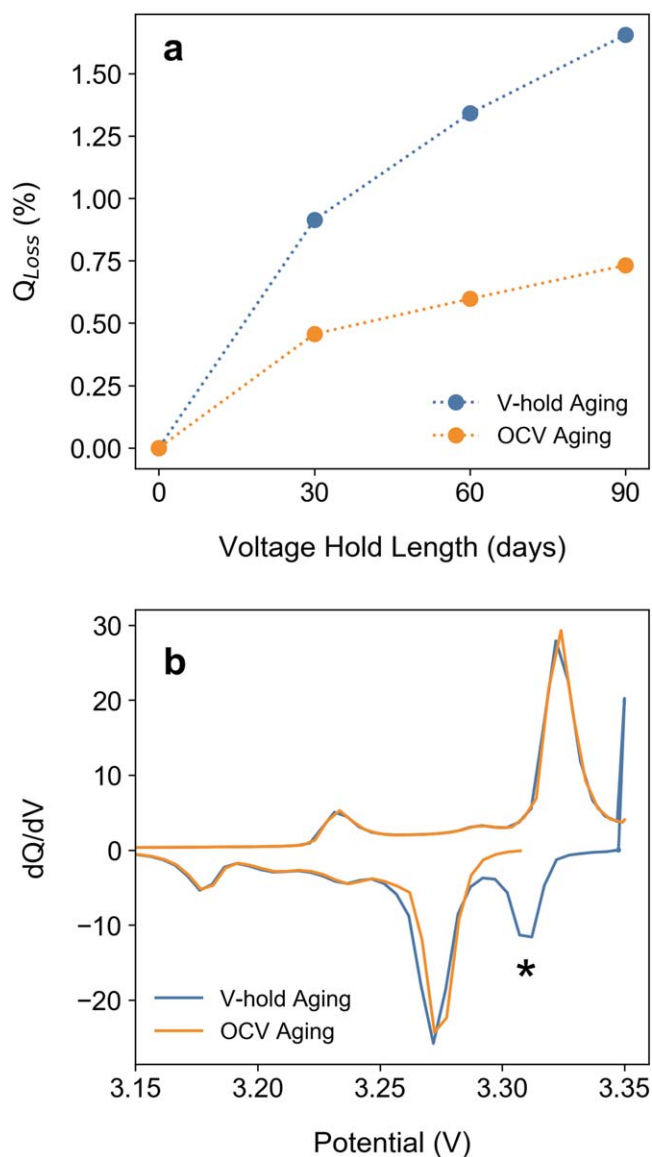
Figure 4. (a) Q_{loss} values vs aging time for Gr-LFP 18650 cells that aged at OCV or during a voltage-hold. (b) Differential capacity traces of Gr-LFP cells aged at OCV or during a voltage-hold. The differential capacity traces are calculated from the lithiation immediately prior to, and the delithiation immediately after the aging period to demonstrate the effect of the aging method on the cell's SOC. The * marks the delithiation peak indicating the cell aging via a voltage-hold reached a higher SOC than the cell aged at OCV, due to the reversible lithiation required to maintain the cell voltage at the hold potential.
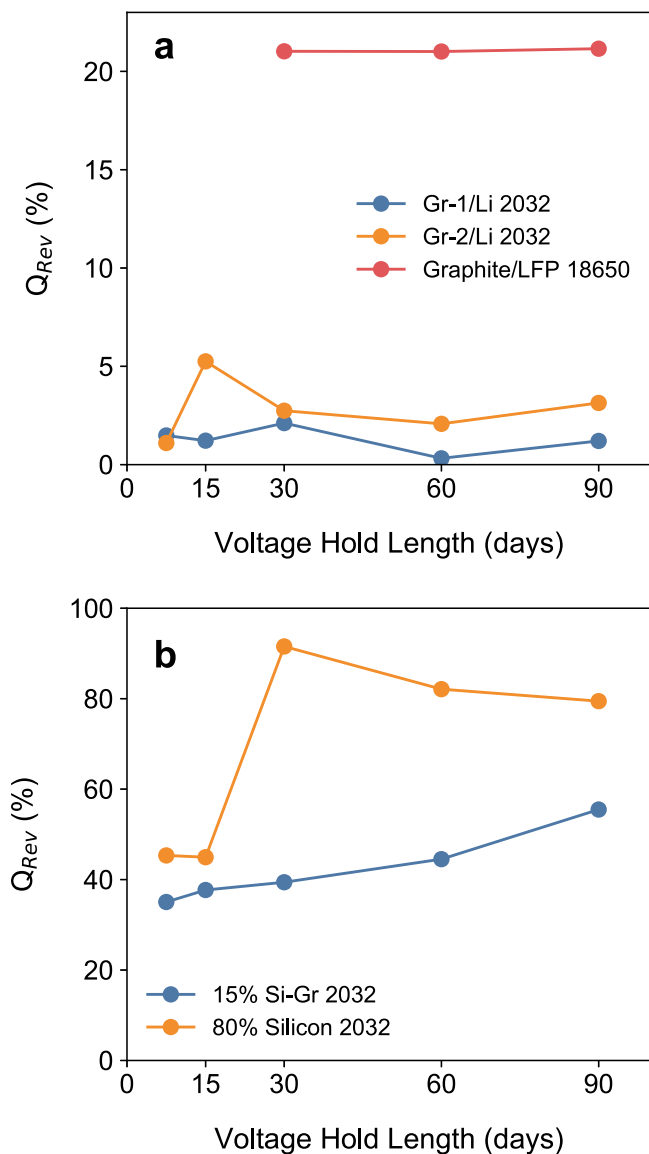
Figure 5. Reversible capacity (Q_{rev}) of different anodes measured during voltage holds, with each data point representing a cell having underwent a voltage hold for 7.5−, 15−, 30−, 60−, or 90 d. (a) The Q_{rev} values of several different graphite-containing cells. Significant differences in Q_{rev} values of the graphite-containing cells between the Li half-cells and the LFP full-cell stem from the graphite electrodes experiencing slight differences in absolute electrochemical potentials during the hold; these effects are detailed in Fig. 10 and related discussion. (b) The Q_{rev} values of various silicon-containing cells.

significant enough that the Q_{rev} was far from negligible ($Q_{rev} = \sim 21\%$). This suggests that choosing an appropriate V_{hold} depending on the anode chemistry is important to minimizing Q_{rev}. Considering that Q_{rev} is non-negligible during a voltage hold, it is important to understand if a voltage hold is long enough for Q_{rev} to reach a maximum, such that I_{rev} becomes negligible compared to the I_{irrev} that is responsible for calendar aging. One simple way to do this is to track values of Q_{rev} for voltage holds of different lengths. Figure 5 shows Q_{rev} values for the commercial 18650 Gr-LFP cells and several other types of cells that underwent voltage holds for varying lengths of time. Figure 5a shows Q_{rev} values of graphite-containing cells that underwent voltage holds between 7.5 and 90 d. Each graphite-containing cell shows little dependency or increase between the shortest and longest hold times, indicating that Q_{rev} has quickly reached a maximum and I_{rev} already becomes negligible for hold times of 7.5 d for the 2032 half-cells and 30 d for the same 18650

lFP cells tested in Fig. 4. Note the graphite-Li half-cells are 2032 coin cells and exhibit some variation in Q_{rev} (on the order of 1%–5%) when tested for different durations. In contrast, the commercial graphite-LFP 18650 cells have rapid and stable relaxation of reversible processes and exhibit a consistent $Q_{rev} = \sim 21\%$, with less than 0.1% variation with test time, showing that the format and quality of assembly of the cell used can have an impact on the consistency of results from voltage hold experiments. All in all, both datasets indicate that Q_{rev} saturates rapidly in graphite cells.

Figure 5b shows Q_{rev} values of silicon-containing 2032 coin cells that underwent voltage holds between 7.5 and 90 d. In contrast to the graphite-only cells, the silicon-containing cells show a general trend of increasing Q_{rev} values (rather than oscillating around a single value) with longer voltage hold times, indicating that I_{rev} is non-negligible even after 90 d. For the Si-graphite electrode (15% Si), the anode gains ~35% of its pre-hold capacity after 1 week of testing and gains another ~25% in the following months. This is likely due to the slow kinetics and large voltage hysteresis of the lithiation and delithiation of silicon, which allows continued reversible lithiation of the silicon for long time periods during a voltage hold. This idea is supported by the larger Q_{rev} values recorded for the silicon-only containing cell in Fig. 5b compared to the mixed silicon-graphite containing cell. These time-dependent voltage hold experiments highlight how the relaxation of the reversible processes (I_{rev}) is dependent on the identity of the electrode being tested. Specifically, active materials exhibiting a large voltage hysteresis (such as silicon) have slow relaxation of reversible lithiation processes, making it challenging to deconvolute the Q_{irrev} component from Q_{rev} during the voltage hold process to forecast calendar aging trends. However, the consistent Q_{rev} values of the graphite cells suggest that they can be promptly investigated using potentiostatic holds.

Another experiment that can be used to assess the timescale of the relaxation of the reversible processes during a voltage hold more easily than the multiple experiments described above is an "inverse polarization" test, which is described in detail in section S2. The inverse polarization experiment simply runs a voltage hold at a potential where delithiation of the anode (rather than lithiation) is the dominant reversible process. This is achieved by first lithiating the anode, resting the cell at open circuit to allow the relaxation of any voltage hysteresis, then delithiating the anode either by a predetermined capacity or until a target potential is reached, at which point a voltage hold is started. The irreversible processes responsible for calendar aging are electrochemical reduction reactions ($I_{irrev} < 0$ in the sign convention of potentiostats) while delithiation is an electrochemical oxidation reaction ($I_{delit} > 0$). The current response during an inverse polarization voltage hold is the sum of these currents:

$$I_{inverse polarization}(t) = I_{irrev}(t) + I_{delit}(t) \qquad [6]$$

Thus, during an inverse polarization experiment, $I_{inverse\ polarization}$ will initially be positive as I_{delit} dominates the current response. As the reversible delithiation processes relax and the irreversible processes start to dominate, $I_{inverse\ polarization}$ will switch signs to become negative (Fig. S2.1a (available online at stacks.iop.org/JES/169/050531/mmedia)). When the current response is zero, the reversible and irreversible processes are equal in magnitude, and continued holding of the voltage will drive $I_{inverse\ polarization}$ to a minimum negative value before it starts to increase back towards zero, as the irreversible processes slowly self-passivate. The time at which $I_{inverse\ polarization}$ reaches a minimum is when $I_{delit} \sim 0$, and the measured current is approximately equal to I_{irrev}; this time serves as a quantitative guide for how long voltage holds must be before they start to yield the desired information on irreversible processes. Examples of typical current responses of inverse polarization experiments are shown in Fig. S2.1. As expected, based on the discussion above, graphite electrodes quickly relax (Fig. S2.1b), while silicon requires hundreds of hours for the residual lithiation to
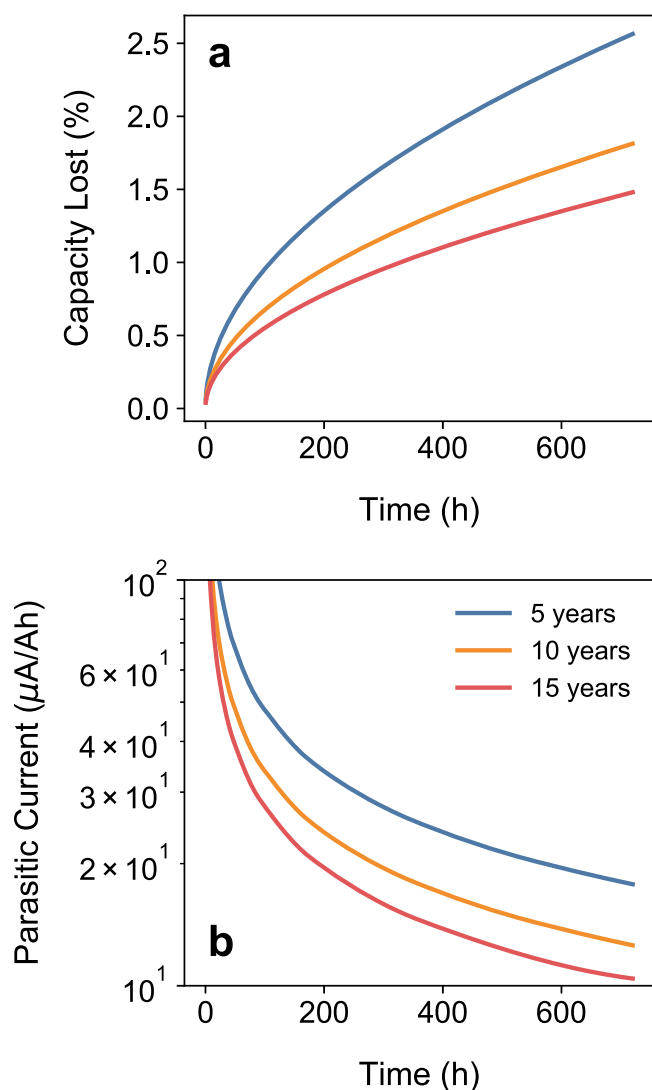
Figure 6. Simulated calendar aging of a hypothetical Li-ion battery assuming a $\sqrt{t}$ time dependency for capacity fade and 5, 10 or 15 years of calendar life (time in which charge loss equals 20% of nominal cell capacity). (a) Capacity loss relative to initial cell capacity. (b) Parasitic current associated with the rate of capacity loss shown in panel a, per Ah of cell capacity. The magnitude of parasitic currents can be sizable for large-format cells. The legend in panel b applies to both panels.

expected during cathode break-in, though comes at the expense of cell health if it continues beyond the initial cycles. This electron transfer effectively *increases* the Li$^+$ inventory of the cathode, causing the perceived capacity fade due to reactions at the SEI to be underestimated. Li-ion batteries stored at open circuit will *lose* capacity over time,[6,25] indicating that the average rate of reduction reactions at the anode surpasses that of oxidation at the cathode. This is partly due to the sloped voltage profile of layered oxide cathodes: electrons gained through oxidation cause a decrease in cathode potential, lowering the driving force for additional oxidation.[32] This is not the case during a voltage hold, as the cathode can deliberately be maintained at high potentials and thus the oxidation reactions can be amplified. This approach has been used in the past to investigate the effect of electrolyte composition on the surface reactivity of cathodes at high voltages,[16,33,34] and was observed to lead to a net *gain* of capacity by the cell,[35] indicating that the rate of oxidation surpassed that of reduction side reactions. The contributions from oxidation processes to cell capacity and the measured currents can be minimized by selecting a cathode with a flat voltage profile (see Fig. 3 and section S1) that remains at low potentials during the voltage hold. A cathode like LFP satisfies both conditions, increasing the ability of the voltage hold technique to track electron exchanges at the anode SEI.

But are these parasitic currents large enough to be measurable in real time? Fig. 6a presents a simulation of the capacity lost by a cell due to calendar aging, assuming a $\sqrt{t}$ dependency; such dependency has been empirically observed in many studies.[5,25,30,36–38] During the first month of aging (720 h), a cell with 15 years of calendar life would lose < 1.5% of its nominal capacity. The derivative of this capacity loss with respect to time is shown in Fig. 6b, indicating the net currents associated with aging processes. After the first month of aging, a cell with 15 years of life would present an instantaneous rate of parasitic reactions of ∼10 µA per Ah of nominal capacity. Translating these values to the currents measured during a voltage hold, the expected magnitudes would be ∼50 nA for a 5 mAh coin cell, 500 nA for a small single-layer pouch cell and >10 µA for commercial batteries. All these values are, in principle, measurable with modern electrochemical instrumentation. However, accurately sensing the currents generated by smaller cells could be challenging for conventional battery cyclers. For illustration, a lab scale Maccor Series 4100 cycler has an accuracy of 75 nA at its lowest current range (< 150 µA), which could measure the currents generated by a 1.2 Ah cell within < 0.63%; deviations for coin cells would be significantly larger. Here, we use 1.2 Ah cylindrical cells to evaluate quantitative aspects of the voltage hold technique, but also discuss how qualitative cell behavior can still be captured in coin cells if the rate of aging of samples is sufficiently distinct. Hardware specifications for all instruments used in this work are provided in Table S3.1.

We note that the sensing accuracy could be problematic even for large-format cells depending on the test settings. Using a Maccor cycler as an example again, the current range needed for C/10 cycling of a 1.2 Ah cell (< 150 mA) would have a current accuracy of only 75 µA. To circumvent this limitation, the tests discussed here were performed using automatic current range selection, which switches the sensing circuitry as the current decays during the voltage hold. An alternative would be to modify the experiment to minimize Q_{rev} and prevent the current from varying across multiple orders of magnitude. This can be achieved by allowing the cell to relax at open circuit prior to the hold and then performing the voltage hold at the post-relaxation OCV (as shown in supplemental section S4).[39] In this case, the test could be performed at a static current range with optimal sensitivity. Naturally, this option requires prior knowledge of the expected current values.

subside (Fig. S2.1c). Thus, voltage hold experiments using silicon-containing electrodes will require much longer times than ones using graphite. It is important to note that the inverse polarization experiment gives information about the timescale of relaxation of reversible *delithiation* processes and may not necessarily be representative of the relaxation of reversible *lithiation* processes during a normal voltage-hold experiment.

How hardware sensitivity and the prominence of reduction reactions can affect voltage holds.—The currents measured during a potentiostatic hold experiment can carry contributions from many processes within the cell that involve an electron exchange. Thus, the technique will only be informative of capacity fade during calendar aging if the rate of parasitic reactions at the SEI is much larger than that of other processes. As discussed in the previous section, continued charging of the cell as it depolarizes is an obvious source of interference, but one that can be overcome by sufficiently long experiments. Another example is oxidation side reactions, which can transfer electrons to the cathode,[31] a phenomenon that is typically

Evaluating whether the anode overhang will affect the measured currents.—The electrochemical activity in a Li-ion cell occurs primarily within the geometric region of the incoming Li$^+$ flux in the electrolyte. Consequently, when the battery is charged, lithiation of
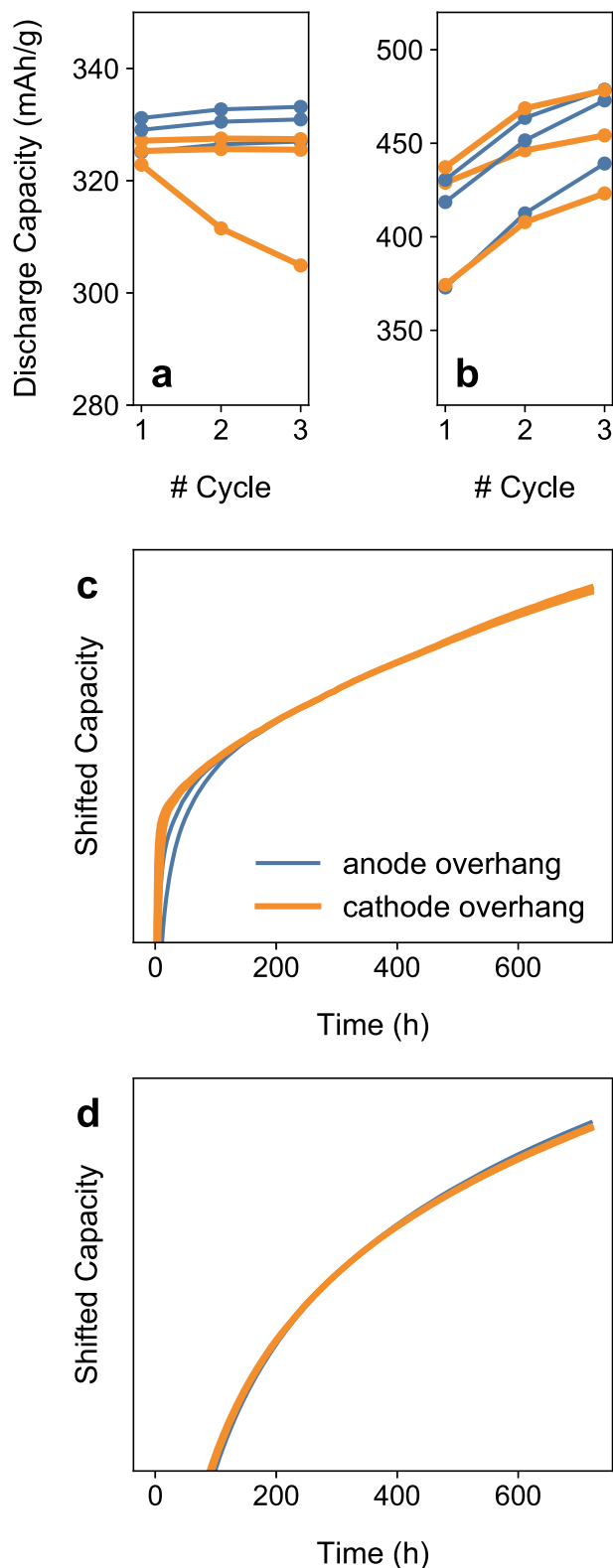
Figure 7. Evaluating the effect of overhang on the trends measured during a voltage hold. (a) Capacities during formation cycles for LFP vs Gr-1 cells with cathode or anode overhang. Capacities are normalized by the weight of active material in the anode. (b) Like panel a, but for LFP vs 15% Si-graphite cells. (c) Shifted normalized capacities exchanged during a voltage hold at 3.35 V of LFP vs Gr-1 cells. (d) Like panel c, but for LFP vs 15% Si-graphite cells. Capacities were arbitrarily shifted to match at 300 h to erase small variations in Q_{rev} and allow a more direct visual comparison of trends. The legend in panel c applies to all panels.

the anode occurs mainly in areas that are directly aligned with the cathode coating. If the two electrodes have identical dimensions, a slight misalignment during cell assembly could decrease their overlapping area, decreasing cell capacity.[40] To minimize the consequences of assembly imperfections, commercial cells typically contain excess anode area, known as "overhang," which improves assembly consistency and decreases the likelihood of Li metal plating.[41] The exact size of this excess area depends on cell format. As an example, Lewerenz et al. recently estimated that the anode was 5.7% larger than the cathode in commercial 8 Ah LFP-Gr cylindrical cells.[42] For research-grade coin cells, geometrically oversizing the anode by ∼15% has been recommended to improve reproducibility.[40]

Although this excess anode area is not the primary destination for Li$^+$ ions, it is also not completely inactive. The overhang is much less prone to undergoing reversible electrochemistry so its SOC will be different from that of the overlapping area. Over time, this gradient will promote the transference of Li$^+$ between central areas of the anode and the overhang.[43,44] Hence, the SOC of the overhang will slowly approach the average cell SOC after extended storage, which can interfere with observations during calendar aging studies.[41,42,44] These interferences could appear as either added charge loss or apparent capacity gain, depending on whether the overhang is initially at a higher or lower SOC than the active anode area.

During a voltage hold in LFP-based cells, electrons are transferred from the cathode to the anode to compensate for the charge lost in the latter. It is possible that the existence of an excess anode area could interfere with the correlation between measured current and rate of parasitic reactions, as the overhang could drain charge from the active area or even be directly lithiated at minute currents. To evaluate the impact of the overhang on potentiostatic hold experiments, we performed tests using identical electrode pairs (LFP vs Gr-1 or LFP vs 15% Si-Gr) but varied which electrode contained the excess area: the anode or LFP. In the single-layer pouch cells used in these studies, the cathode had a larger areal capacity than the anode (N/P ratio < 1), to guarantee that the cathode would remain in the flat portion of the LFP voltage profile during the test, even at high anode SOCs and after accounting for the irreversible losses during the initial formation cycles. The near-constant LFP potentials and the slow cycling rates also helped eliminate the risk of Li plating along the anode edges in the presence of a cathode overhang. All cells had a nominal active area of 14.1 cm^2, which is the area of the smaller electrode that is directly underneath the larger 14.9 cm^2 counter electrode, with a total of 5.4% of overhang excess.

All cells were exposed to three formation cycles at C/10 (2.7–3.42 V for Gr-1 and 2.7–3.35 V for Si-Gr), and then charged to 3.335 V and held at this potential for 720 h (one month). During the formation cycles, we observed that LFP-Gr-1 cells with anode overhang had 1%–3% higher capacity than the ones with cathode overhang (Fig. 7a), indicating that a fraction of the excess area appears to be readily accessible during cycling. These general trends were also observed with 15% Si-Gr anodes, although the cell-to-cell variability presented similar magnitude (Fig. 7b). During the voltage hold, cells with anode overhang tended to require longer times to achieve a steady behavior (Fig. 7c), which could also be indicative of lithiation of excess anode areas. However, once this initial behavior subsided, all cells presented identical rates of capacity exchange (Figs. 7c, 7d), suggesting that the existence of an anode overhang did not appear to significantly affect the trends measured within the duration of these voltage hold experiments. If these results can be generalized, they indicate that the observations obtained with this technique may not be adversely impacted by the existence of excess anode area, making voltage holds compatible with state-of-art cell assembly methods.

Can voltage holds provide accurate quantitative predictions of calendar aging?.—The previous sections indicated that, under the

correct conditions, potentiostatic holds could provide information about the rate of parasitic reactions at the SEI. If the technique accurately measures this rate in real time, then it would potentially be able to *quantitatively predict* the calendar life of cells as limited strictly by Li$^+$ inventory loss at the anode, as suggested in Fig. 2d. One direct approach to assess the accuracy of the method is to directly compare the irreversible capacity measured during a voltage hold (Q_{irrev}) with the actual loss calculated from the cycles before and after the hold (Q_{loss}). An agreement between these two values would indicate that parasitic processes are correctly measured, and that reversible and irreversible currents can be properly distinguished. Figure 8 walks through the comparison between $Q_{hold}(t)$, $Q_{irrev}(t)$, and Q_{loss} for commercial Gr-LFP 18650 cells, with Fig. 8a showing an example voltage profile of the experiments. These cells are the same ones used in Fig. 4 and provide a stable system for proof of concept of quantitative analysis capability. Importantly, the irreversible capacity passed during the voltage hold can be calculated by rearranging Eq. 1:

$$Q_{irrev}(t) = Q_{hold}(t) - Q_{rev}(t) \qquad [7]$$

where $Q_{rev}(t)$ is the increase in SOC during the voltage hold as discussed in Fig. 4b. At sufficiently long times, $Q_{rev}(t)$ ideally becomes a constant rather than a function of time, and can thus be calculated as a total value passed by the end of the voltage hold (Q_{rev}, Eq. 5). Figure 8b shows the raw data of the $Q_{hold}(t)$ and the true capacity loss (Q_{loss}, Eq. 4) calculated from the surrounding cycles. Figure 8c shows $Q_{irrev}(t)$ with the reversible capacity ($Q_{rev} = {\sim}21\%$ and is constant for the times considered in the commercial 18650 cells, Fig. 5a) subtracted from $Q_{hold}(t)$ measured during the hold. It is clear that Q_{irrev} overestimates the capacity loss at all cases, and that this error grows with test time. Consequently, Q_{irrev} grows with time much faster than Q_{loss} (Fig. 8d), indicating that any extrapolation of the measured voltage hold data would lead to a large overestimate of the actual calendar aging rate of the cell. Indeed, attempts to fit and extrapolate the voltage hold data assuming
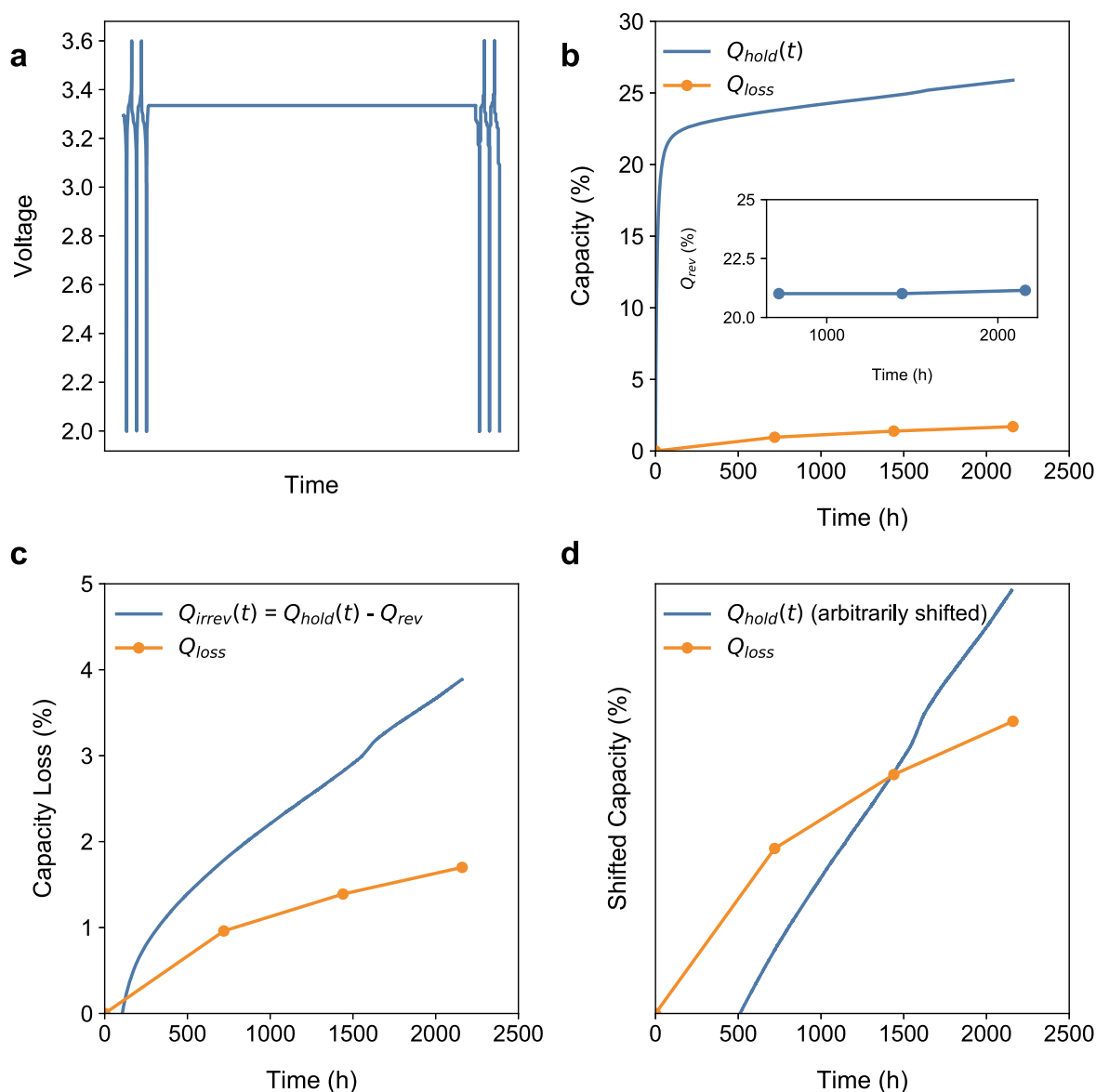

Figure 8. (a) Potential profile of voltage hold experiment run on the Gr-LFP 18650 commercial cells. The voltage holds were done at 3.35 V. (b) Capacity loss measured during 90 d V-hold (Q_{hold}) and capacity loss measured using the RPT and forming cycles of 3 separate cells aged for 30−, 60−, and 90−d, respectively (Q_{loss}). Capacity loss values are shown as a percentage of the last forming cycle discharge capacity of each cell ($Q_{cycle\ 3\ discharge}$). The reversible capacities (Q_{rev}) shown in the inset plot are determined by subtracting the charge capacity immediately prior to the voltage hold from the discharge capacity immediately after the voltage hold. (c) Capacity measured during 90 d V-hold with the 90 d Q_{rev} value subtracted (Q_{irrev}). (d) Shows Q_{hold} arbitrarily shifted to directly compare trends with Q_{loss}. Q_{hold} exhibits a greater slope further indicating the overestimate of loss compared to the actual loss, Q_{loss}.
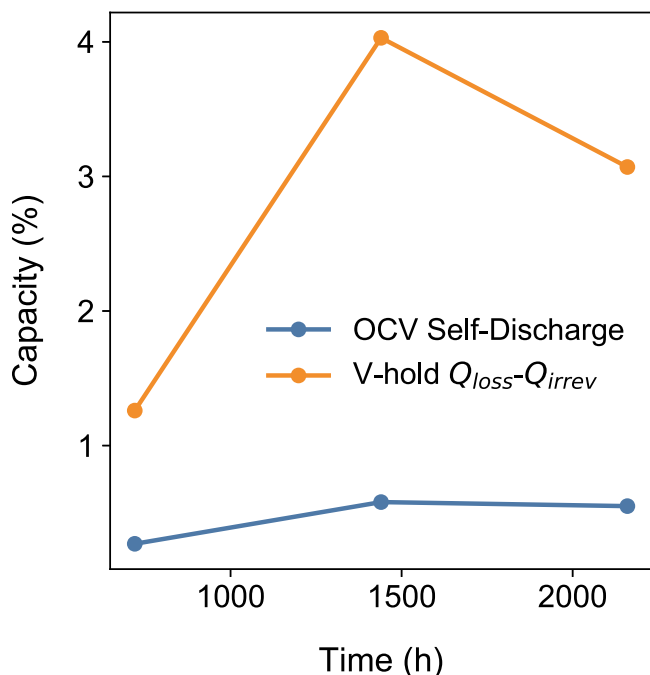
Figure 9. Comparison of the reversible self-discharge measured during 30, 60, and 90 d OCV rests and the excess capacity measured during 30, 60, and 90 d 3.35 V voltage holds of commercial LFP-Gr 18650 cells. The values for OCV rest cells were calculated by taking the difference between Q_{loss} (calculated using Eq. 4) and the perceived loss (calculated using the charge/discharge before/after the OCV aging step). The values for the V-hold cells were calculated by taking the difference between Q_{loss} (calculated using Eq. 4) and Q_{irrev} (calculated from Eq. 7). In the case of OCV rest cells, the values shown represent reversible self-discharge while in voltage hold cells, which are pinned at a set voltage (and SOC), the values shown are excess capacity from reversible processes that are not fully understood. The capacities were normalized to the delithiation before the hold.

common functional forms used in the literature to describe time-dependent degradation consistently resulted in unexpectedly low calendar lives (Fig. S5.1). These observations strongly suggest that, unfortunately, the voltage hold test may lack quantitative utility.

Such a discrepancy between Q_{irrev} and Q_{loss} could be explained by the following: i) parasitic currents are consistently overestimated by the sensing hardware; ii) there could be additional processes contributing to the measured current. Section S3 shows that the expected error based on typical instrument specifications would be less than 0.2% of the cell capacity for a month-long hold of these commercial cells, which cannot explain the more than 3% disparity between Q_{irrev} and Q_{loss} in Fig. 8c. Therefore, we hypothesize that additional processes contributing to the measured current must be responsible for the observed discrepancies. We next consider the nature of these processes.

One possibility is that the reversible (anode lithiation) contributions to the measured capacity could remain significant over the duration of the voltage hold, causing the irreversible (parasitic) contributions responsible for calendar aging to be overestimated. However, the inset in Fig. 8b shows that Q_{rev} as a function of hold time is relatively constant (< 0.5% variation with no clear trends, which could be caused by small cell-to-cell differences) and therefore, reversible charging is unlikely to be the source of extra capacity. Furthermore, as seen in section S4, when an OCV relaxation is performed prior to the voltage hold, reversible lithiation is minimized but the long-term trends are still like a voltage hold without an OCV step before it. This further proves that reversible lithiation cannot be the only source of excess capacity.

Yet another possible process is that the large overestimate of irreversible reactions during the voltage hold may also be due to *reversible capacity loss*. One example of such processes is charge

exchange with the anode overhang, which we ruled out based on the data shown in Fig. 7. Another possibility is the contribution of reversible self-discharge processes. During traditional calendar aging experiments in which cells are allowed to age at open circuit (as in Fig. 4), it is commonly observed that the discharge immediately after the storage period overestimates the true capacity fade. Processes such as electrolyte oxidation and redox shuttles during long-term storage can temporarily decrease cell SOC without causing permanent loss of Li$^+$ inventory,[32,41,45,46] causing cell capacity to rebound in subsequent cycles. It is conceivable that these temporary losses are included in the charge measured during the voltage hold, leading to artificially high fade rates. From the cells charged to 3.35 V and stored at open circuit (Fig. 4), we can estimate the reversible self-discharge by taking the difference between the perceived loss (the difference between the discharge and charge immediately after and before the aging step, respectively) and Q_{loss} (calculated using Eq. 4). For the open circuit cells, the reversible self-discharge is less than 0.6% for all test durations (Fig. 9) indicating that reversible self-discharge does not completely explain the greater than 3% difference between Q_{hold} and Q_{loss} in Fig. 8c. Similar calculations for cells tested using voltage holds (the difference between Q_{loss}, Eq. 4 and Q_{irrev}, Eq. 7) resulted in even higher capacity values (1%–4% depending on time). Unlike cells stored at OCV, voltage hold cells are pinned at the setpoint voltage of 3.35 V. Therefore, reversible self-discharge processes should manifest as excess capacity rather than a decrease in voltage as with OCV reversible self-discharge. Comparing the magnitude of this excess capacity during the voltage hold in Fig. 9 with the difference between Q_{hold} and Q_{loss} in Fig. 8c, reversible processes leading to excess capacity could be a significant, but perhaps not the only, contributor to the overestimated capacity loss. The cause of this reversible excess capacity during the voltage hold is not fully understood, though is clearly greater than the analogous reversible self-discharge capacity during OCV aging. Due to the presence of additional processes besides reversible charging (Q_{rev}, anode lithiation) and parasitic processes, a better description of the total capacity exchanged during the potentiostatic hold may be:

$$Q_{hold}(t) = Q_{irrev}(t) + Q_{rev,charging}(t) + Q_{other\ rev.processes}(t) \qquad [8]$$

Without a better understanding of this third term, quantitative prediction of calendar aging is difficult. The lack of quantitative behavior in the voltage hold of well-behaved commercial Gr-LFP cells will translate to research-grade systems where the same issues will be present, and possibly exacerbated due to complexities in different potential profiles and increased variability.

Can voltage holds resolve semi-quantitative calendar aging trends?.—In the previous section, we demonstrated that potentiostatic holds fall short of perfectly quantifying the electron exchanges that lead to Li$^+$ inventory loss. Even though non-idealities in electrode profiles could theoretically cause underestimation of instantaneous parasitic currents (Section S1), the previous section showed that the opposite behavior occurs in reality: the measured rate of side reactions was consistently larger than the actual rate of parasitic processes. Although a quantitative analysis seems out of reach of this technique, semi-quantitative information could still be available if the errors are reasonably systematic (i.e., if deviation is nearly constant across various testing conditions). Semi-quantitative analyses could still be very useful for accelerating calendar aging studies, as they provide estimates of the degrees of improvement among a set of variables, such as voltage, SOC and electrolyte composition.

To evaluate the merits of potentiostatic holds for semi-quantitative analysis, we once more resorted to commercial 18650 format LFP-Gr cells to serve as reproducible model systems. The cells were received with an OCV of ~3.292 V and presented initial C/10

discharge capacities of 1182 ± 9 mAh. Cells were refrigerated shortly after being received to prevent calendar aging, with select cells being warmed up for testing (at 25 °C). A total of 8 cells were charged to and held at 3.24, 3.26, 3.292, 3.32, 3.335 and 3.35 V for 720 h (30 d), with duplicates at 3.292 and 3.335 V; the test protocol was like the protocol illustrated in Fig. 8a. The equilibrium SOCs achieved after relaxation during the hold at these voltages are shown as "x" in Fig. 10a. These SOCs could differ significantly from that exhibited at the same voltage during constant current cycling (CC, ▲ in Fig. 10a), with the departure depending on the proximity to plateaus in the full-cell profile. With depolarization, cells can gain a significant amount of capacity as plateaus become accessible, making the magnitude of Q_{rev} strongly dependent on the hold voltage (Fig. S5.2). The final SOC after the initial relaxation during the hold is equal to the capacity during the CC charge plus Q_{rev}. As

clear from Fig. 10a, the cell tends to move away from plateaus after the initial relaxation.

The Q_{loss} observed for all cells and the measured Q_{irrev} are shown in Fig. 10b. Just as discussed in the previous section, Q_{irrev} was observed to be consistently *larger* than the actual amount of capacity that is lost by the cells, and this gap appears to become larger at higher voltages. Interestingly, cells tested at 3.24 and 3.26 V actually *gained* capacity after the voltage hold (i.e., they displayed a negative loss in Fig. 10b), while cells at 2.292 V were at the threshold of gaining/losing charge. This type of behavior (capacity gain during calendar aging at low voltages) has been reported previously and has been ascribed to charge being driven out of the overhang areas and distributing across the bulk of the anode, which is at a lower average SOC than the overhang.[41–44] Since the cells were received at ∼3.292 V, the overhang is presumably at an SOC corresponding
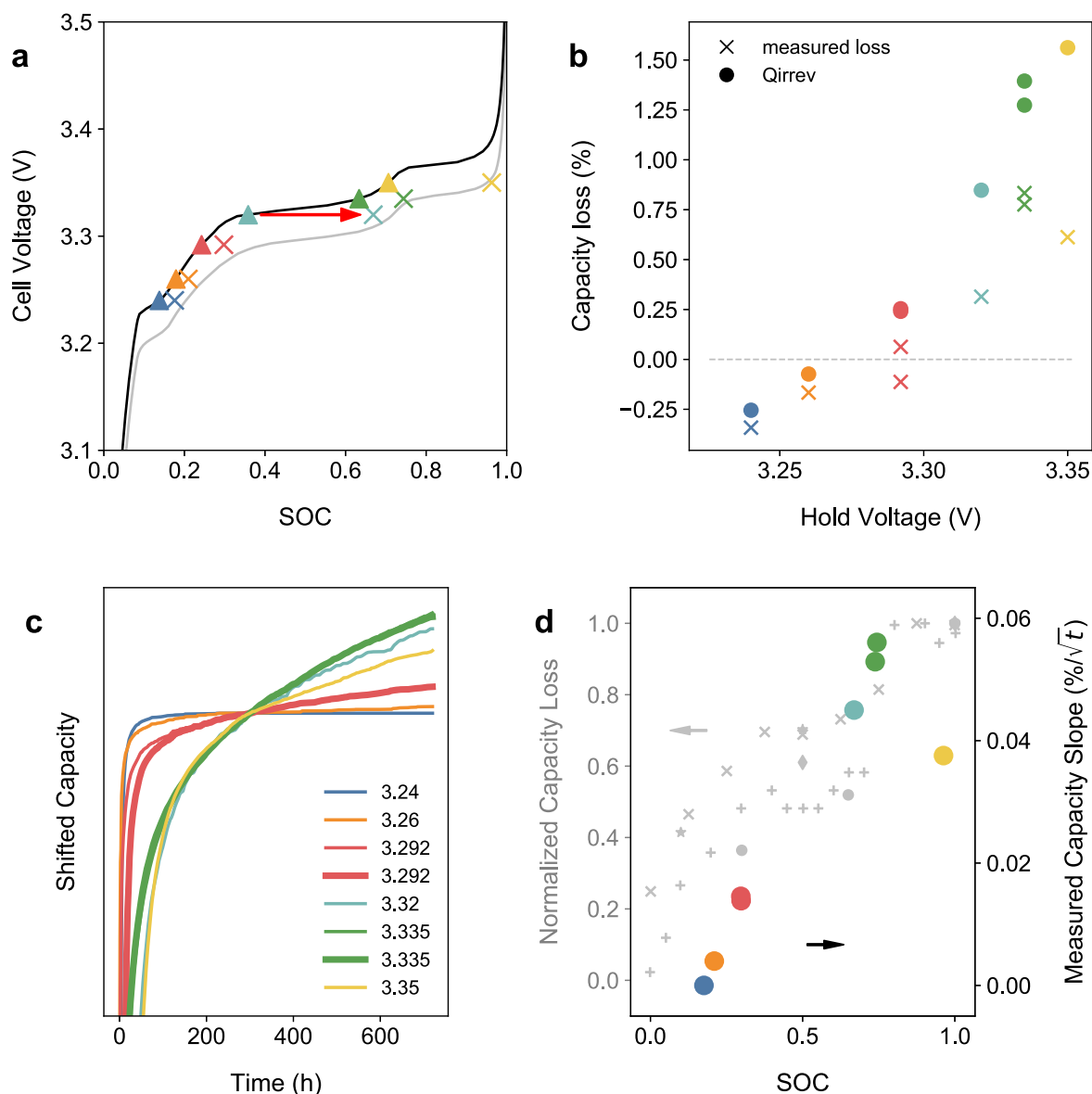

Figure 10. Potentiostatic holds of LFP-graphite cylindrical cells at various voltages. (a) SOC of the cell immediately before the voltage hold (▲) and at the end of the voltage hold (x). During the hold, the cell SOC grows by a factor equal to Q_{rev}, which can be particularly large at the vicinity of plateaus as charge can be exchanged at small voltage increments. The black voltage profile was obtained at C/10 during charge, while the gray curve is a pseudo-OCV obtained by averaging C/10 charge and discharge profiles. Although the pseudo-OCV does not provide an exact picture of the cell SOC after the hold, it is a good approximation, especially at high SOCs. (b) Q_{irrev} (•) and actual capacity loss (x) as a function of hold voltage. Capacity loss was calculated using Eq. 4. All values are normalized by the initial full capacity of the respective cells. (c) Integrated capacity exchanged during the potentiostatic hold. Values were normalized by the initial capacity of each cell, and then shifted vertically to present identical values at t = 300 h. (d) Rates of aging extracted from the voltage holds (colored circles, right axis) and normalized capacity fade. Data shown as gray symbols indicate the normalized total capacity loss measured at each SOC, as reported in the following works: • (Ref. 51), x (Ref. 5), + (Ref. 25), ★ (Ref. 55), ◆ (Ref. 56). The legend in panel c applies to all panels.

to that potential, and the near zero losses observed at 3.292 V supports the hypothesis of the overhang being the source of this behavior. The fact that the measured exchanged capacity is larger than the actual loss irrespective of the aging potential relative to the initial cell OCV again negates major contributions of the overhang to the trends measured during voltage hold within this timeframe of one month.

The capacities exchanged during the hold at all voltages, each normalized by the respective cell capacity, are shown in Fig. 10c. The capacity curves were vertically shifted to have identical values at t = 300 h, to ignore the contribution of Q_{rev} and allow better visual comparison of the trends. The tests presented remarkable reproducibility, as exemplified by the identical behavior of the sets tested at 3.292 and 3.335 V. In most cases, aging is faster (that is, the

capacity curves visibly display a higher rate of capacity loss) at higher cell potentials, in agreement with the known trends of SEI growing faster at higher SOCs. A clear exception is the cell held at 3.35 V, which is discussed in detail below.

To attempt to quantify these aging trends, we used the terminal slope of capacity vs $\sqrt{t}$ ($\sqrt{h}$) plots as proxy for the rate of calendar aging, as satisfactory linear fits were obtained for most datasets (see Fig. S7.3). The fitted slopes are shown in Fig. 10d (filled circles). Also included in this figure is data from various sources in the literature indicating the normalized capacity fade during calendar aging studies of LFP-Gr cells. The symbols are clearly arranged in the traditional S-shape of the plateaus of graphite; SOCs within a plateau exhibit a similar anode potential, and thus a similar driving force for reduction reactions, leading to similar aging rates.[25,30] If
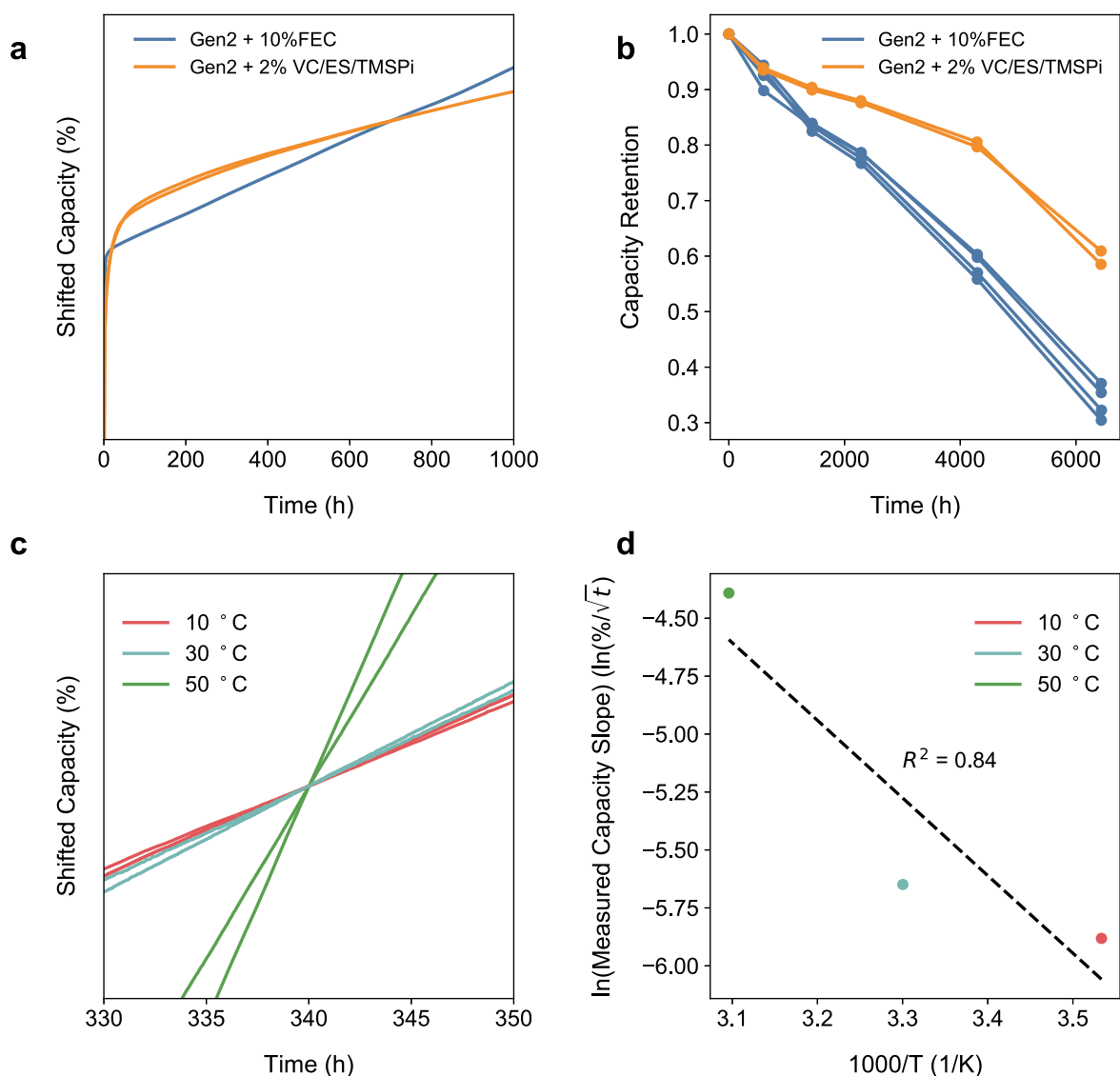

Figure 11. Example of qualitative behavior of the voltage hold. (a) Shows the voltage hold of graphite-1 anodes and LFP cathodes with electrolytes of Gen2 + 10% FEC and Gen2 + 2% VC + 2% ES + 2%TMSPi at 3.335 V in 2032 coin cells recorded on Maccor battery cyclers. The curves are shifted to account for differences in reversible lithiation and their local slopes are compared at 700 h and were normalized to the charge capacity directly before the hold. A greater slope indicates a larger parasitic current suggesting worse calendar life in the Gen2 + 10% FEC electrolyte. (b) Depicts the calendar aging comparison of the two electrolytes with the same graphite electrode against NMC622 in 2032 coin cells. Three reference performance cycles were performed every ∼720 h of OCV rest starting at 4.1 V. Capacity retention is calculated from the last delithiation of the RPTs relative to the final delithiation of formation cycles prior to calendar aging. Consistent with the voltage hold, the larger negative slope of the Gen2 + 10%FEC electrolyte indicates worse performance. Rapid fade for both systems may have been caused by unreasonably large anode overhang and/or reactivity of coin cell parts. (c) Shows the voltage hold of Gr-2 vs LFP with Gen2 + 10% FEC electrolyte at 3.335 V at 10 °C, 30 °C, and 50 °C. The expected trends of increasing slope, indicating increasing parasitic processes, is observed going from 10 °C to 50 °C. (d) Shows the approximate correspondence of the temperature data with the Arrhenius relationship. The slopes of the capacity vs $\sqrt{t}$ were taken from 150 to 360 h for the y axis values. The agreement of the OCV measurements and voltage hold experiments along with the correct qualitative behavior of the temperature data provides a proof of concept of the qualitative ability of the voltage hold.

the voltage hold can accurately resolve the semi-quantitative relationship between aging rates at various SOCs, the filled circles in Fig. 10d should coincide with the gray symbols. Figure 10d provides two main observations: i) the slopes extracted from potentiostatic holds generally follow the expected *qualitative* progression, but not necessarily with quantitative exactitude; ii) the test at 3.35 V largely underestimates the rate of aging. In section S7 of the *Supplemental Material* we provide a detailed discussion about the origin of this behavior. Briefly, it can be traced back to the fact that, at 3.35 V, the cell is no longer at the plateau portion of the LFP voltage profile (see Fig. 10a), causing aging to induce constant shifts in the electrode potentials over time that consequently lead to the measured current underestimating the rate of parasitic processes. Once that is accounted for, the correct *qualitative* trends can be obtained (see Fig. S7.4b), though they remain inaccurate for *quantitative* purposes.

Overall, our studies indicate that comparative aging trends can be directly assessed when experiments are performed within a flatter portion of the cathode profile (such as all voltages except for 3.35 V in Fig. 10). More generally, it appears that the correct *qualitative* trends can be obtained when the relative slopes of the voltage profiles of the cathode and anode are accounted for (as shown in section S7). Nevertheless, even after correction of the aging rates, the *quantitative* relationship between rates observed at all SOCs does not follow the expected trends; that is, the measured aging rates do not rigorously follow the path traced by the gray symbols in Fig. 10d. These observations suggest that potentiostatic holds may be limited to providing qualitative information about parasitic processes. Further exploration of the qualitative aspect of the technique is provided in the next section.

Can voltage holds provide qualitative information about calendar aging?.—In the previous section, we showed that the qualitative aging rates recorded during potentiostatic holds at different voltages followed the expected trends of higher parasitic currents at higher SOCs. Despite the quantitative limitations of the technique, this observation suggests that voltage holds could be useful for the fast screening of materials and compositions. This could accelerate the discovery of new methods to improve calendar aging by quickly identifying promising systems, that can then be validated in long-term RPT-based aging experiments or future rapid quantitative methods described in Fig. 1b. This section will show additional qualitative validation of the voltage hold technique.

A second example of potentiostatic holds correctly capturing the qualitative aging behavior of cells is shown in Fig. 11. The relative trends observed in the voltage hold should correspond to the same trends in more traditional calendar aging experiments when new materials are compared to a baseline. The best performing material would therefore be the one with the shallowest slope for capacity lost during both the voltage hold and during more traditional calendar aging at open circuit. An example of this for the comparison between electrolytes for a graphite electrode is shown in Figs. 11a, 11b. The Gen2 + 10% FEC electrolyte shows a greater rate of capacity fade in both the voltage hold at 3.335 V and traditional OCV calendar aging compared to the electrolyte containing Gen2 + 2% VC + 2% ES + 2% TMSPi. This demonstrates the qualitative use of the voltage hold since the voltage hold and OCV trends both indicate the same electrolyte formulation decreases the calendar aging rate of the same electrode type. Importantly, note how this conclusion is already evident < 200 h into the voltage hold, which is significantly faster than the time interval covered by the first few RPTs in Fig. 11. As discussed above, this time advantage is easily accessible for systems that exhibit fast current relaxation, such as graphite.

A third example of correct qualitative behavior is shown in Figs. 11c, 11d. It is widely reported in the literature that higher temperatures will exacerbate parasitic processes and thus accelerate the calendar aging of LIBs.[6,25,47–50] Figure 11c shows the exchanged capacity measured during the voltage hold of LFP vs Gr-2 coin cells

at 3.335 V at 10, 30 and 50 °C. Curves were normalized and vertically shifted, and only a portion of the data is shown for clarity. Tests at higher temperatures yielded capacity curves with higher slopes, consistent with a thermal acceleration of aging processes. Furthermore, direct extraction of aging rates (from capacity vs $\sqrt{t}$ plots, as in Fig. 10d) resulted in reasonable linearity of an Arrhenius plot (Fig. 11d), in agreement with previous studies on the effect of temperature on calendar aging.[51–53] This finding agrees with the work of Lewerenz et al., that also observed an Arrhenius dependency in currents measured during voltage holds at various temperatures.[19]

These examples further demonstrate the validity of using voltage holds for qualitative comparisons of the rate of reactions at the SEI across different systems (electrolyte additives) and experimental conditions (temperature and voltage). However, caution must be taken during experiment design to ensure reliable results. As we noted above, differences between material performances during the voltage hold may be subtle, especially for smaller cell formats in which parasitic currents approach the hardware detection limits. Due to the higher variability inherent with research-grade cells, replicates are highly recommended to correctly identify relative trends; additionally, pouch cells tend to present superior reproducibility to more common coin cells. We emphasize that voltage holds should be used to guide the initial down selection of promising systems based on the stability of the SEI layer, and that the technique does not replace traditional long-term experiments, such as the one used by the United States Advanced Battery Consortium (USABC) that utilizes an OCV-RPT style test.[9] Certain aging mechanisms, such as the ones involving loss of accessible active material, will only become evident after such extended experiments.

A quick guide to using voltage holds for qualitative screening.—Important considerations for using voltage holds for qualitative comparisons to predict calendar life are summarized in Table II. Three of the most important variables for the correct qualitative use of voltage holds include: (i) sufficient lithium inventory; (ii) sufficient time to allow reversible processes to relax; and (iii) a carefully chosen voltage.

The protocol used in this paper was designed to only evaluate lithium inventory loss to the SEI. For obtaining reliable results, the cathode must present a large enough lithium supply that is accessible with negligible potential variation. This way, reactions at the SEI and reversible lithiation processes can draw from this supply during the voltage hold while maintaining the electrodes at constant potentials. If the counter electrode does not contain sufficient lithium, a drop in current during the voltage hold may occur, leading to an erroneous conclusion about the quality of the SEI (Figs. 12a, 12b). This artifact is caused by the cathode shifting away from a SOC range with a flat voltage profile, causing the anode SOC to vary during the test and the parasitic processes to be underestimated (see section S1). More specifically, we recommend that tests should be done with LFP counter electrodes in such a way that the entire voltage hold is still within the LFP plateau. Therefore, the total capacity required (from both reversible and irreversible processes, along with initial SEI formation) must be understood. In commercial LFP-Gr cells, the rate of capacity loss is slow enough that voltage holds with cells with N/P ratio > 1 are still possible. In research-grade coin cells, however, excess cathode capacity and electrolyte may be necessary to prevent inventory exhaustion.

Qualitative voltage holds will only be accurate if the recorded electron exchanges are primarily due to parasitic processes rather than reversible lithiation. The longer the voltage hold, the more likely this is to be true since reversible relaxation should have asymptotic behavior and subside over time. During experiment design, an inverse polarization test can be used to estimate the relaxation time of reversible processes (see section S2). Aging trends should therefore be considered only at times much greater than the relaxation time indicated by inverse polarization experiments. The slow relaxation of reversible processes is demonstrated in Fig. 12c

Table II. Considerations for successfully implementing qualitative voltage hold comparisons to infer relative calendar life performance.

Steps	Considerations
Preparation	• Inverse polarization experiments can be performed to determine necessary voltage hold time to allow reversible lithiation relaxation
	• Consider choice of test voltage to ensure different anodes are at similar potentials, enabling comparison between different systems
	• Select type of instrument (cycler or potentiostat) and its current range setting to accurately measure the currents expected from the size (capacity) of the cells being tested
Performing the experiment	• Cathode must have flat voltage profile
	• Cathode must supply sufficient Li^+ inventory to remain at SOCs where its voltage profile is flat during the entire voltage hold experiment
	• Perform voltage hold sufficiently long to relax reversible lithiation as dictated by inverse polarization results
Data analysis	• Plot both hold current and capacity to make trends more clear
	• Compare trends of capacity plots after removing reversible lithiation contributions
	• Make replicates to ensure observed trends are valid
	• Greater consistency may be achieved with pouch cells as compared with coin cells
Limitations	• The method only probes lithium inventory loss, not other degradation mechanisms
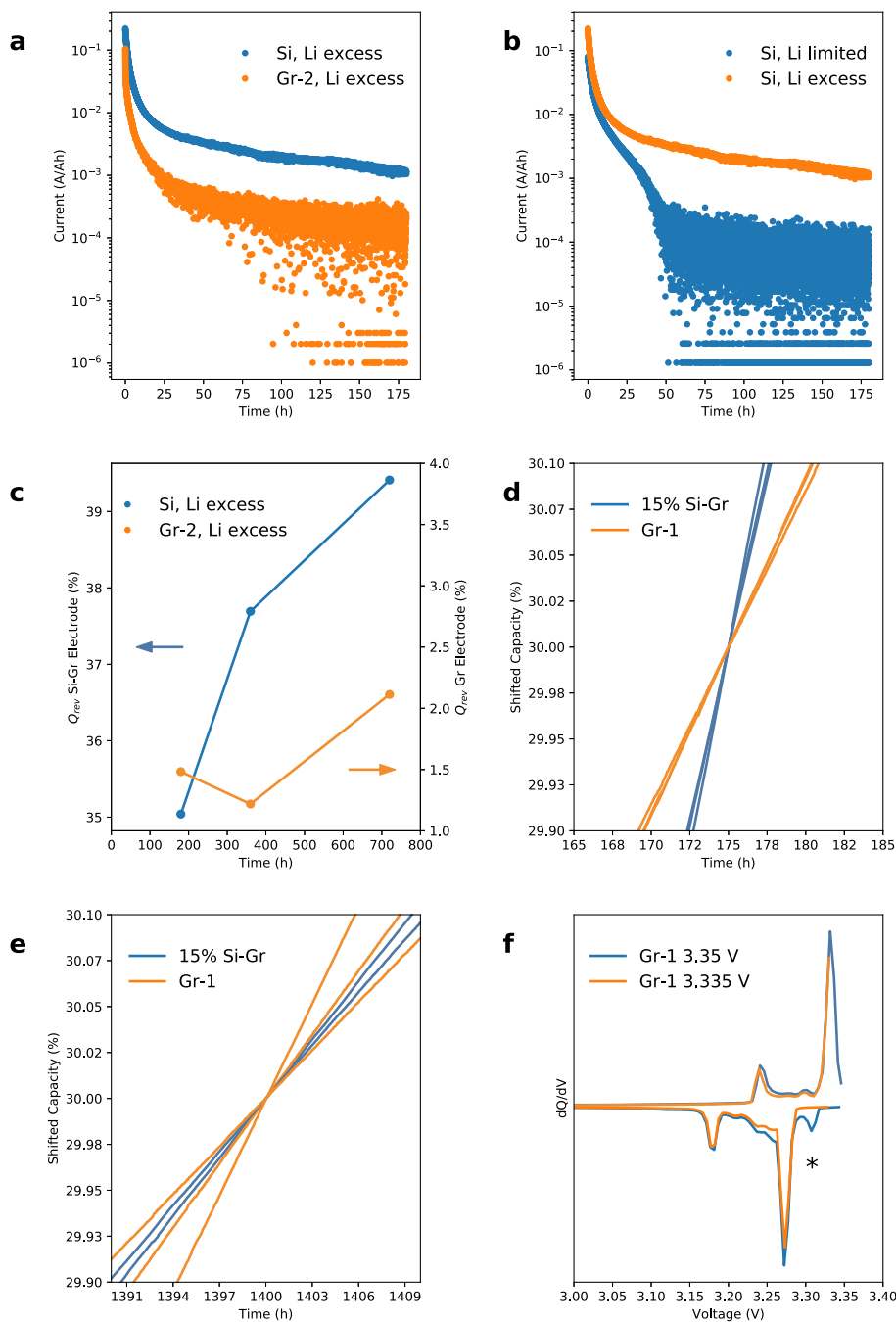
Figure 12. The major variables that need to be considered to make good qualitative comparisons of voltage hold data include sufficient lithium inventory to support all reversible and irreversible processes, sufficient time to allow parasitic processes to dominate over reversible processes, and careful choice of voltage hold potential. All data shown is from 2032 coin cells and data was acquired on Maccor battery cyclers. (a) Shows an example of a 180 h voltage hold at 100 mV vs Li/Li$^+$ of a silicon and graphite-2 electrode half-cell with sufficient lithium inventory while (b) shows a 180 h voltage hold of the same silicon electrode with (Li counter electrode) and without (LFP counter electrode) sufficient lithium inventory. The potential at the anode in both cases was approximately 100 mV vs Li/Li$^+$. The drop in current in the limited lithium case represents the exhaustion of the lithium inventory rather than a decrease in parasitic processes and results in a lower current than the excess lithium case. (c) Shows the reversible capacity passed as a function of voltage hold length at 3.35 V for a Si-Gr and Gr-2 electrode against a lithium counter electrode. The reversible capacity increases with time for the silicon indicating the reversible processes still have not relaxed after a 720 h hold. Conversely, the reversible capacity of the Gr remains relatively stable with voltage hold length suggesting more facile relaxation. The current in (a) for Si is greater than Gr, but this could just be because the reversible processes have not yet relaxed and are a major contributor to the voltage hold capacity as depicted in (c). (d) and (e) provide an example of the importance of hold length on making qualitative performance comparisons of hold capacity plots at different times. The cells shown are Gr-1 and 15% Si-Gr electrodes vs LFP with Gen2 + 10% FEC in 2032 coin cells. The capacity plots are arbitrarily shifted to make slope comparisons. In (d) graphite at 175 h clearly has a smaller slope than Si-Gr, but in (e) at 1400 h, the difference between the two is far more subtle since the silicon has had more time for reversible processes to relax. (f) shows the effect of voltage choice on a graphite-1 electrode (vs LFP). The lithiation in the dQ/dV is prior to the voltage hold and the delithiation is after a 720 h voltage hold at either 3.35 or 3.335 V. At 3.35 V, the final plateau of graphite starts to lithiate during relaxation, which is evident by the peak shown during delithiation at approximately 3.31 V (labeled with *). If the voltage is adjusted to 3.335 V, the last plateau is not lithiated during the hold and the 3.31 V peak is absent during delithiation. The choice of potential will directly influence the contribution of reversible current during the voltage hold which can convolute comparisons between different electrodes.

for an 80% Si electrode, where the reversible capacity as a function of voltage hold length increases after 720 h, indicating the electrode has still not reached equilibrium. Graphite, on the other hand, remains relatively stable at ∼1.5% regardless of voltage hold length, suggesting much faster relaxation kinetics. Hence, the data shown in Fig. 12a is insufficient to assess the relative rates of capacity loss across both anodes, as much of the current for Si arises from reversible lithiation rather than side reactions. In other words, an electrode with slow lithiation kinetics will also lead to a more persistent reversible current contribution, increasing the observed current during the hold. The importance of this point is further highlighted in Figs. 12d, 12e, using LFP vs Gr-1 and LFP vs 15% Si-Gr cells. When comparing the capacity trends after only 175 h into the hold, the Gr electrode looks much superior to the Si-Gr anode, as evident from the smaller slope of the capacity curve. However, if the same cells are compared after 1400 h, the difference between the two data sets becomes much more subtle. At the beginning, the current is dominated by reversible current, so the silicon electrode, with slower lithiation kinetics, will appear to perform worse. This demonstrates the importance of having a sufficiently long voltage hold even for qualitative comparisons. We note that the determination of the time necessary for an electrode to relax and be dominated by parasitic current is difficult. Although the inverse polarization experiments can suggest approximate times, we performed these experiments in

half-cells and under delithiation conditions, so it must be assumed that the times determined under these conditions are representative of and are transferrable to full-cells under anode lithiation conditions. An option to help decrease hold time would be to have an OCV step prior to the voltage hold, with the voltage after relaxation being used as the hold voltage; this minimizes reversible lithiation during the hold so qualitative comparisons can be made more quickly (Section S4).

Finally, it is important to consider the choice of test voltage. Since reversible lithiation will occur early during the hold, the effective cell SOC during the test will differ from the one immediately prior to the hold. This is exemplified in Fig. 12f by the dQ/dV curves of the charge and discharge before and after the potentiostatic hold, respectively, for a commercial LFP vs Gr 18650 cell. When the cell is initially charged to either 3.335 V or 3.35 V, the anode potential is approximately ∼120 mV vs Li/Li$^+$, as can be inferred from the sharp peak in the differential capacity profile at those potentials. However, the SOC of each cell will progress differently during the voltage hold. When held at 3.35 V, the anode will be lithiated down to the ∼89 mV vs Li/Li$^+$ plateau of graphite (see the new delithiation peak at 3.31 V, labeled *), while the anode potential is insufficient to lithiate graphite to its second plateau potential when held at a cell voltage of 3.335 V. In addition to extending the time needed for reversible processes to relax, the 3.35 V scenario will also expose the cell to a flatter region of the anode profile, which can affect the ability of the test to accurately measure reduction reaction rates (see section S1). Also, reaching an anode plateau increases the likelihood of exhausting the inventory of the cathode, causing artifacts such as the ones discussed in Figs. 10d and 12b. Although it is difficult to determine the effective SOC during the hold without prior knowledge, we found that using pseudo-OCV profiles provided reasonable success; see Fig. 10a for details. Considering test voltage can be particularly important when comparing anodes containing different active materials (Si vs graphite, for example). Since the driving force for reduction reactions is proportional to the anode potential, the chosen cell voltage must be as equivalent as possible between different anodes. This common anode potential should ideally be in regions in which the slopes of both voltage profiles is much higher than that of the cathode, to improve the sensitivity of the technique to measuring SEI processes.

Although the recommendations above improve the reliability of experiments, care must also be taken when analyzing the data. In the discussion above, we either compared systems through inspecting the visual trends of exchanged capacities over time (Fig. 11c), or directly extracted slopes from capacity curves after trends remained linear for hundreds of hours (Fig. S7.3). Both procedures ensure that aging can be judged based on general future trends, rather than on an instantaneous behavior. Shifting curves vertically to eliminate the contribution of Q$_{rev}$ is also useful to facilitate visualization. The progression of measured currents is often less clear and less robust (see section S6), and thus is not directly used in our analyses.

Despite the utility of the voltage hold for the fast qualitative screening of materials, it does have limitations. The technique provides information on lithium inventory loss but does not explicitly capture other degradation mechanisms such as the loss of active material due to electrical isolation which has been reported in commercial Si-Gr electrodes.[41,54] The conditions of the voltage hold are also important, and adequate thought must be given to the potentials of the voltage hold experiments to make fair comparisons between different electrodes. Additionally, voltage hold duration must be sufficiently long to resolve parasitic current trends without being overshadowed by reversible current, and materials with poor kinetics may require very long experiments. Lastly, the approach taken in this paper focuses on understanding calendar life changes due to either electrolytes or electrode materials that affect the stability of the SEI on the anode. Hence it cannot be directly extended to studying the effect of cathodes on the system due to the difference in voltage profiles of different cathodes. For example, the
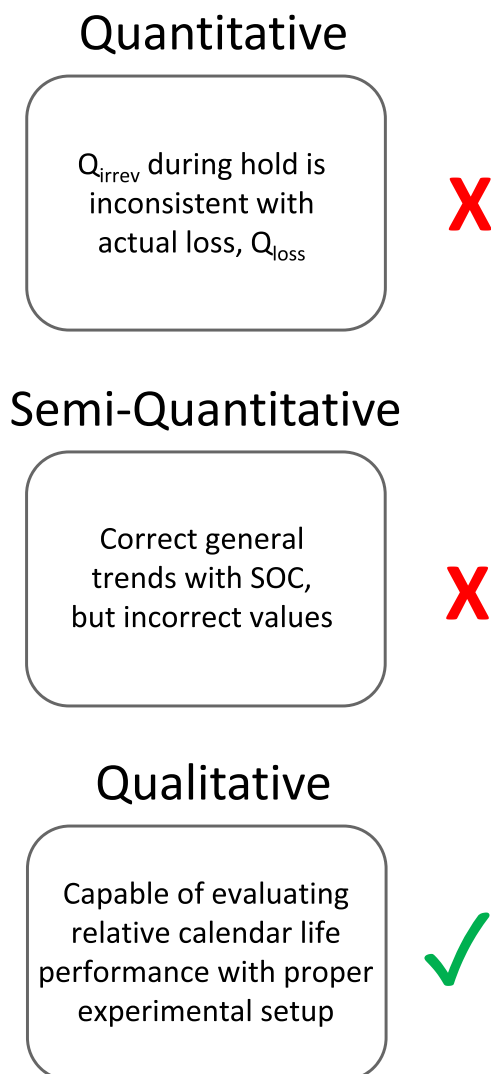
Quantitative

Q$_{irrev}$ during hold is inconsistent with actual loss, Q$_{loss}$ ✗

Semi-Quantitative

Correct general trends with SOC, but incorrect values   ✗

Qualitative

Capable of evaluating relative calendar life performance with proper experimental setup   ✓

Figure 13. Summary of results for quantitative, semi-quantitative, and qualitative application of the voltage hold to evaluate calendar life performance.

use of an NMC cathode for a voltage hold will lead to a shift in the anode profile with lithium loss and also introduce oxidative instability of the electrolyte as a variable, further convoluting the meaning of the measured current. Such data would thus not be directly comparable to the data acquired from tests using LFP counter electrode, even if the same anode was held at the same effective potential. Finally, results from voltage hold tests were observed to be much more consistent when using formats that are larger than conventional coin cells. The use of pouch cells is encouraged when possible, and replicates are necessary to ensure that real trends are observed. Occasionally, differences in performance between two systems may be too subtle to be reliably measured using short voltage holds, requiring conventional long-term testing for a complete assessment.

Conclusions

Decreasing the rate of calendar aging has important practical relevance for the mass deployment of Li-ion batteries, as capacity fade due to parasitic reactions at the SEI can affect the economic feasibility of many applications. Since this time-dependent aging is the cumulative effect of very slow processes, studying and mitigating these phenomena can be extremely resource-intensive. Hence, creating methods that can quickly assess future aging trends is needed to support the development and validation of new active materials and electrolyte additives.

This manuscript discussed whether potentiostatic holds can be used for such purposes and the results are summarized in Fig. 13. When cells are maintained at a certain voltage for an extended time, the residual charging eventually subsides and the measured current then becomes indicative of the rate of parasitic electron exchanges occurring at the electrodes. We show that, if experiments are performed with the cathode maintained at relatively low and invariant potentials (such as in the case of $LiFePO_4$), then the measured current becomes extremely sensitive to reduction reactions at the anode. Thus, in principle, potentiostatic holds could allow the direct measurement of the time dependency of electron and Li^+ losses to the SEI and could quickly provide a description of calendar aging trends. Our work explored experiments in various cell formats to evaluate the quantitative power of this technique.

Our studies indicated that the exchanged capacity recorded during the voltage hold consistently overestimated the real capacity loss experienced by the cells during the experiment, exhibiting faster aging trends than expected for the cell chemistry. Moreover, this deviation did not seem to arise from a systematic error, as the relative aging rates exhibited by cells tested at different SOCs did not reproduce the well-established quantitative behavior observed for graphite anodes. The deviation was also observed to increase with increasing hold times, suggesting that errors were both SOC- and time-dependent. Nevertheless, the qualitative trends observed in these tests were generally correct: cells tested at higher SOCs (and thus held at lower effective anode potentials) exhibited faster rates of aging. We further offered two additional examples of success of the voltage hold technique in identifying qualitative trends, by showing the effect of temperature and electrolyte composition on calendar aging. These observations suggest that this method can be used as a screening tool, highlighting formulations and conditions that could deliver improved calendar life. This initial screening would help decrease the parameter space of longer aging studies, optimizing the allocation of resources and improving the likelihood of a successful outcome.

We also explored whether the fundamental assumption that charging currents will eventually vanish during the hold was correct. We described how inverse polarization assays could be used to estimate the relaxation times for anode materials and demonstrated that silicon could have significantly slower kinetics than traditional graphite electrodes, even in thin films. Consequently, Si would require long voltage hold experiments for the results to be truly descriptive of aging behavior. Alternatively, we note that analysis of the early current decay of Si-based cells could be an effective tool to evaluate how improvements in electrode and electrolyte composition improve the kinetics of Si.
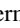
While this study focused on the use of LFP as a counter electrode, we recognize that this is not the case with typical high-energy cells. The favored layered oxide cathodes typically present sloped voltage profiles, which generally makes voltage tests more sensitive to oxidation than to reduction side reactions. While correlating the measurements using these cathodes with capacity fade is difficult, these tests still represent the rates of *some* parasitic process and can still provide useful insights if carefully designed.

We expect that the present work will provide battery scientists and developers with a solid base upon which to build and that future work with improved instrumentation and varying test conditions could expand the capabilities of this method. More importantly, we hope this work helps emphasize the need for designing tools that can expedite the cycle of innovation in the battery field.

ORCID

Marco-Tulio F. Rodrigues https://orcid.org/0000-0003-0833-6556
Daniel P. Abraham https://orcid.org/0000-0003-0402-9620
Ira Bloom https://orcid.org/0000-0002-4877-473X
Alison R. Dunlop https://orcid.org/0000-0001-9785-0375
Gao Liu https://orcid.org/0000-0001-6886-0507
Stephen E. Trask https://orcid.org/0000-0002-0879-4779
Gabriel M. Veith https://orcid.org/0000-0002-5186-4461
Ankit Verma https://orcid.org/0000-0002-7610-8574
Christopher Johnson https://orcid.org/0000-0003-4357-6889

References

1. M. Winter, B. Barnett, and K. Xu, *Chem. Rev.*, **118**, 11433 (2018).
2. G. He, R. Ciez, P. Moutis, S. Kar, and J. F. Whitacre, *Appl. Energy*, **273**, 115151 (2020).
3. Z. Liu, J. Song, J. Kubal, N. Susarla, K. W. Knehr, E. Islam, P. Nelson, and S. Ahmed, *Energy Policy*, **158**, 112564 (2021).
4. K. Xu, *Chem. Rev.*, **104**, 4303 (2004).
5. M. Naumann, M. Schimpe, P. Keil, H. C. Hesse, and A. Jossen, *J. Energy Storage*, **17**, 153 (2018).
6. M. Dubarry, N. Qin, and P. Brooker, *Curr. Opin. Electrochem.*, **9**, 106 (2018).

7. E. V. Thomas, I. Bloom, J. P. Christophersen, and V. S. Battaglia, *J. Power Sources*, **206**, 378 (2012).
8. J. E. Harlow et al., *J. Electrochem. Soc.*, **166**, A3031 (2019).
9. U.S. Department of Energy Vehicle Technologies Program, *United States Advanced Battery Consortium Battery Test Manual For Electric Vehicles, Revision 3.1*, (2020), https://cet.inl.gov/ArticleDocuments/USABCElectricVehicleTestManualRev3.1.pdf.
10. T. Gewald, M. Lienkamp, D. Lehmkuhl, and A. Hahn, *14th International Conference on Ecological Vehicles and Renewable Energies (EVER), Institute of Electrical and Electronics Engineers Inc.* (2019).
11. C. L. Seitzinger et al., *Chem. Mater.*, **32**, 3199 (2020).
12. R. T. Pekarek et al., *J. Mater. Chem. A*, **8**, 7897 (2020).
13. B. Han, Y. Zhang, C. Liao, S. E. Trask, X. Li, R. Uppuluri, J. T. Vaughey, B. Key, and F. Dogan, *ACS Appl. Mater. Interfaces*, **13**, 28017 (2021).
14. J. D. McBrayer et al., *Nat. Energy 2021*, **69**, 866 (2021).
15. A. Tornheim, S. E. Trask, and Z. Zhang, *J. Electrochem. Soc.*, **163**, A1717 (2016).
16. A. Tornheim, J. C. Garcia, R. Sahore, H. Iddir, I. Bloom, and Z. Zhang, *J. Electrochem. Soc.*, **166**, A440 (2019).
17. K. Kalaga, M. T. F. Rodrigues, S. E. Trask, I. A. Shkrob, and D. P. Abraham, *Electrochim. Acta*, **280**, 221 (2018).
18. N. R. Vadivel, S. Ha, M. He, D. Dees, S. Trask, B. Polzin, and K. G. Gallagher, *J. Electrochem. Soc.*, **164**, A508 (2017).
19. M. Lewerenz, S. Käbitz, M. Knips, J. Münnix, J. Schmalstieg, A. Warnecke, and D. U. Sauer, *J. Power Sources*, **353**, 144 (2017).
20. M. Theiler, C. Endisch, and M. Lewerenz, *Batteries*, **7**, 22 (2021).
21. A. Zülke, Y. Li, P. Keil, R. Burrell, S. Belaisch, M. Nagarathinam, M. P. Mercer, and H. E. Hoster, *Batter. Supercaps*, **4**, 934 (2021).
22. S. S. Zhang, *J. Energy Chem.*, **41**, 135 (2020).
23. H. Zhang, H. Liu, L. F. J. Piper, M. S. Whittingham, and G. Zhou, *Chem. Rev.*, **122**, 5641 (2022).
24. H. Gao et al., *Nano Lett.*, **17**, 1512 (2017).
25. P. Keil, S. F. Schuster, J. Wilhelm, J. Travi, A. Hauser, R. C. Karl, and A. Jossen, *J. Electrochem. Soc.*, **163**, A1872 (2016).
26. M. C. Schulze, G. M. Carroll, T. R. Martin, K. Sanchez-Rivera, F. Urias, and N. R. Neale, *ACS Appl. Energy Mater.*, **4**, 1628 (2021).
27. M.-T. F. Rodrigues, J. A. Gilbert, K. Kalaga, and D. P. Abraham, *J. Phys.: Energy*, **2**, 024002 (2020).
28. M. Wetjen, S. Solchenbach, D. Pritzl, J. Hou, V. Tileli, and H. A. Gasteiger, *J. Electrochem. Soc.*, **165**, A1503 (2018).
29. W. M. Dose, V. A. Maroni, M. J. Piernas-Muñoz, S. E. Trask, I. Bloom, and C. S. Johnson, *J. Electrochem. Soc.*, **165**, A2389 (2018).
30. F. Single, A. Latz, and B. Horstmann, *ChemSusChem*, **11**, 1950 (2018).
31. A. Tornheim and D. C. O'Hanlon, *J. Electrochem. Soc.*, **167**, 110520 (2020).
32. R. Jung, M. Metzger, F. Maglia, C. Stinner, and H. A. Gasteiger, *J. Electrochem. Soc.*, **164**, A1361 (2017).
33. A. Tornheim, S. Sharifi-Asl, J. C. Garcia, J. Bareño, H. Iddir, R. Shahbazian-Yassar, and Z. Zhang, *Nano Energy*, **55**, 216 (2019).
34. A. Tornheim, M. He, C.-C. Su, and Z. Zhang, *J. Electrochem. Soc.*, **164**, A6366 (2017).
35. M.-T. F. Rodrigues, K. Kalaga, S. E. Trask, I. A. Shkrob, and D. P. Abraham, *J. Electrochem. Soc.*, **165**, A1697 (2018).
36. J. Schmalstieg, S. Käbitz, M. Ecker, and D. U. Sauer, *J. Power Sources*, **257**, 325 (2014).
37. P. M. Attia, W. C. Chueh, and S. J. Harris, *J. Electrochem. Soc.*, **167**, 090535 (2020).
38. P. Gasper, K. Gering, E. Dufek, and K. Smith, *J. Electrochem. Soc.*, **168**, 020502 (2021).
39. Y. Yin et al., *ACS Appl. Mater. Interfaces*, **12**, 26593 (2020).
40. B. R. Long et al., *J. Electrochem. Soc.*, **163**, A2999 (2016).
41. I. Zilberman, J. Sturm, and A. Jossen, *J. Power Sources*, **425**, 217 (2019).
42. M. Lewerenz, J. Münnix, J. Schmalstieg, S. Käbitz, M. Knips, and D. U. Sauer, *J. Power Sources*, **345**, 254 (2017).
43. B. Gyenes, D. A. Stevens, V. L. Chevrier, and J. R. Dahn, *J. Electrochem. Soc.*, **162**, A278 (2015).
44. R. Burrell, A. Zulke, P. Keil, and H. Hoster, *J. Electrochem. Soc.*, **167**, 130544 (2020).
45. C. Delacourt and M. Safari, *J. Electrochem. Soc.*, **159**, A1283 (2012).
46. R. Spotnitz, *J. Power Sources*, **113**, 72 (2003).
47. F. Leng, C. M. Tan, and M. Pecht, *Sci. Rep.*, **5**, 1 (2015).
48. Y. Wu, P. Keil, S. F. Schuster, and A. Jossen, *J. Electrochem. Soc.*, **164**, A1438 (2017).
49. I. Bloom et al., *J. Power Sources*, **101**, 238 (2001).
50. C. Stetson, Y. Yin, C. S. Jiang, S. C. Decaluwe, M. Al-Jassim, N. R. Neale, C. Ban, and A. Burrell, *ACS Energy Lett.*, **4**, 2770 (2019).
51. S. Grolleau, A. Delaille, H. Gualous, P. Gyan, R. Revel, J. Bernard, E. Redondo-Iglesias, and J. Peter, *J. Power Sources*, **255**, 450 (2014).
52. M. Ecker, J. B. Gerschler, J. Vogel, S. Käbitz, F. Hust, P. Dechent, and D. U. Sauer, *J. Power Sources*, **215**, 248 (2012).
53. S. L. Hahn, M. Storch, R. Swaminathan, B. Obry, J. Bandlow, and K. P. Birke, *J. Power Sources*, **400**, 402 (2018).
54. X. Li, A. M. Colclasure, D. P. Finegan, D. Ren, Y. Shi, X. Feng, L. Cao, Y. Yang, and K. Smith, *Electrochim. Acta*, **297**, 1109 (2019).
55. D. Li, D. L. Danilov, J. Xie, L. Raijmakers, L. Gao, Y. Yang, and P. H. L. Notten, *Electrochim. Acta*, **190**, 1124 (2016).
56. M. Safari and C. Delacourt, *J. Electrochem. Soc.*, **158**, A1123 (2011).